ETH
Eidgenössische Technische Hochschule Zürich
Swiss Federal Institute of Technology Zurich

Mixed bilinear Raviart-Thomas and triangular linear finite elements virtual gap technique applied to Poisson's equation

Semester Paper

Tanja Almeroth

December 31, 2016

Advisor: Prof. Dr. Ralf Hiptmair
Seminar for Applied Mathematics, ETH Zürich

Abstract

This semester paper gives the preparatory work for a numerical approximation of Poisson's equation with a Dirichlet boundary condition in two dimensions. A mixed finite element approach is applied to the primal-dual coupling problem. Conforming bilinear lowest-order Raviart-Thomas elements are imposed on the primal domain and conforming triangular linear finite elements on the dual domain. Basis functions of both finite element spaces and the stiffness matrix elements are derived. Applying the virtual gap technique the basis is scaled in order to maintain a well-posed linear system. The focus is on deriving all formula in order to implement the method in a straight forward manner in the MATLAB finite element toolbox LehrFEM.

Contents

Acknowledgments

I want to thank my advisor Prof. Dr. Ralf Hiptmair for the opportunity of doing this work and his advise. Also, I give thanks to my friend Carlos Parés Pulido for proofreading my semester paper.

Chapter 1

Introduction

This work is sought to solve Poisson's problem computationally in a charge free region, which occurs in electrostatics [6, chp. 1, eq. 1.38]. The partial differential equation is also known as the Laplace equation with a Dirichlet boundary condition [1].
It is specified in terms of the *primal-dual problem*, by splitting the domain of definition $\Omega \subset \mathbb{R}^2$ and equipping the primal variable with a Dirichlet boundary condition, respectively the dual variable with a Neumann boundary condition, on the joint boundary as in the work [15] by Wieners and Wohlmuth. Motivated by practical interest in applications, introducing several adjacent sub domains, is a concept used in acoustics and electromagnetism modeling [5]. For example a domain can have differing material parameters on sub domains.
Poisson's equation is formulated as *weak solution*, namely the *saddle point problem* [2], [15]. *Sobolev spaces* are the standard functional analysis framework of the imposed numerical methods (e. g. [3], [11], [15], [9]). The occurring Sobolev spaces are L^2, which is the 0th order Sobolev space, the 1st order Sobolev space of functions vanishing on $\Gamma \subseteq \partial\Omega$ and $H(div;\Omega)$.
This variational problem is sought to be solved numerically using a discretization by *mixed finite elements* [2, chp. 2.1.4], developing the two sub domains approach from [15] to multiple. Finite elements (FEM) are triplets (K, Π, Σ), as [3] defines. In contrast to [15] in this work besides triangular, bilinear and triangular FEMs are used. For the triangular case $K = T$, a triangle [3]. We use triangular linear FEMs. In the bilinear case $K = R$, a rectangle [11] and mixed piecewise constant FEMs and Raviart-Thomas FEMs as given in [2] are used. Since like Wieners and Wohlmuth in [15] we apply a *conforming method*, the continuity assumptions enforced to the corresponding FEM spaces, build up from the the polynomial spaces Π, differ for each of the three FEM types. The definitions imposed in this work follow the book [2]. Simultaneously the technique for deriving a basis of the finite

element spaces differ. Based on the idea of Bahriawati and Carstensen in [1], who state a basis of triangular Raviart-Thomas FEM, a basis is derived. Our main technical tool of verifying results are affine transformations like found in the literature [11] and [3]. A linear system arises, when using a basis of the finite dimensional FEM spaces.
Assuming the *primal domain* has a "zero-width" and separates the others, is promising in the development of efficient simulations [5]. Applying this *virtual gap technique*, the linear system is ill-posed, therefore it is regularized by scaling. The matrix of the scaled linear system, called the *stiffness matrix*, is derived in the following with the aim of implementing the imposed method in the MATLAB Finite Elements toolbox LehrFEM.
The contributions of the scaled stiffness matrix, whose entries correspond to edges on rectangles of zero with or height, are stencils. A different approach leads to similar patterns, using bilinear Raviart-Thomas FEM on square elements [7]. Due to the limitation of the scope of this work our stencil is not further analyzed in order to relate it with respect to certain material properties or modifying it, while maintaining sparsity and convergence properties.

This work is organized as follows: In chapter 2 the governing problem equations of Poisson's problem and a brief introduction to Sobolev spaces are given. FEMs are elaborated in chapter 3 and in chapter 4 the stiffness matrix of the model equation of this work is stated.

1.1 Notation

In this work the following notations and aberrations are used:

- Vector valued functions and variables are denoted by $\mathbf{q} = (q^1, q^2, ..., q^d)^\intercal \in \mathbb{R}^d$. $\mathbf{q}^\intercal$ denotes the transposed of a vector.
- μ denotes the Lebesgue measure.
- $L^\infty(\Omega)$ denotes the space of essentially bounded measurable functions on Ω, an open subset of $\mathbb{R}^d$.
- $L^2(\Omega)$, for Ω an open subset of $\mathbb{R}^d$, denotes the Hilbert space of complex measurable functions with the inner product $\langle f, g\rangle_{L^2(\Omega)} := \int_\Omega \bar{f} g \quad d\mathbf{x}$ for $f, g : \Omega \mapsto \mathbb{C}$, where $\bar{f}$ denotes the complex conjugate of f.
- $C^0(\Omega)$ denotes the space of continuous functions $f : \Omega \to \mathbb{R}$.
- $C^\infty(\Omega)$ denotes the space of smooth functions on $f : \Omega \to \mathbb{R}$.
- $C_0^\infty(\Omega)$ denotes the subspace of $C^\infty(\Omega)$, containing compactly supported functions.
- For $v \in H$, H a Hilbert space, v^* denotes the dual with respect to $\langle \cdot, \cdot \rangle_H$, the inner product on H.

- $conv\{A_1, A_2, ..., A_n\}$ denotes the convex hull of $A_1, A_2, ..., A_n \subset \mathbb{R}^d$.
- $|A| = \mu(A)$ denotes the volume, area or length for $A \subset \mathbb{R}^d$.

Chapter 2

Statement of the Problem

This chapter formulates the Poisson's equation in a strong and weak sense.

2.1 Continuous Problem

The problem from [15] is stated as in the following.

Let Ω be in $\mathbb{R}^2$, a bounded domain with polygonal boundary $\partial\Omega$ and f a function in $L^2(\Omega)$. A scalar, elliptic Dirichlet problem [3, chp. 2, sec. 2, eq. 2.5] is given by

$$Lu := -\mathrm{div}(A\nabla u) + bu = f \quad \text{in} \quad \Omega \quad \text{and} \tag{2.1a}$$

$$u = 0 \quad \text{on} \quad \partial\Omega. \tag{2.1b}$$

The following assumptions are made on the above boundary value problem (BVP). A is a symmetric, uniformly positive definite matrix valued function, in particular, $A = (A_{ij})_{i,j=1}^2$, where $A_{i,j} \in L^\infty(\Omega)$ for all $1 \leq i, j \leq 2$ and b is an essentially bounded and non-negative function, i. e. , $0 \leq b \in L^\infty(\Omega)$. The domain of definition $\overline{\Omega}$ is divided into two sub domains $\overline{\Omega_p}$ and $\overline{\Omega_d}$, such that Ω_i are polyhedral for $i = p, d, \overline{\Omega} = \overline{\Omega_p} \cup \overline{\Omega_d}, \mu(\partial\Omega_d \cap \partial\Omega) \neq 0$. They are called *primal* and *dual* domain in the following. The joint boundary is denoted by $\Gamma = \partial\Omega_p \cap \partial\Omega_d$ and the dual boundary $\Gamma_d = \partial\Omega \cap \partial\Omega_d$. An illustration of the partition can be found in figure 2.1.

On Ω_p the following mixed BVP is imposed with a Dirichlet boundary condition on Γ

$$Lu_p = f \quad \text{in} \quad \Omega_p, \tag{2.2a}$$

$$u_p = u_d \quad \text{on} \quad \Gamma \quad \textit{and} \tag{2.2b}$$

$$u_p = 0 \quad \text{on} \quad \partial\Omega_p \setminus \Gamma, \tag{2.2c}$$

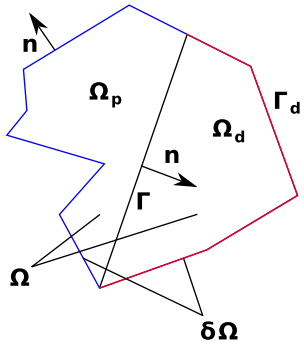

Figure 2.1: Partition of the domain of definition.

where u_d is the *weak solution* on Ω_d. A definition of the weak solution can be found in section 2.2.2. u_p is called the *primal variable*. Whereas on Ω_d the mixed BVP is imposed for the so called *dual variable* u_d:

$$Lu_d = f \quad \text{in} \quad \Omega_d, \tag{2.3a}$$
$$\mathbf{n} \cdot \nabla u_d = \mathbf{j_p} \cdot \mathbf{n} \quad \text{on} \quad \Gamma \quad \text{and} \tag{2.3b}$$
$$u_d = 0 \quad \text{on} \quad \Gamma_d, \tag{2.3c}$$

where $\mathbf{j}_p$ is the flux in Ω_p and $\mathbf{n}$ is the outwards pointing normal unit vector of the primal domain. Note that the flux in Ω_p is given by

$$\mathbf{j}_p = A \nabla u_p. \tag{2.4}$$

2.2 Weak Problem

In the following the function spaces in order to state the space of solutions to the problem (2.1) - (2.3) are introduced. Beginning with *Sobolev spaces* (def. 2.1), the *trace theorem* (thm. 2.4) is particularized, $H(div;\Omega)$ (eq. (2.11)) and *weak solutions* are defined (def. 2.8) for the purpose of giving the *saddle point problem* in section 2.2.2.

2.2.1 Sobolev Spaces and $H(div;\Omega)$

As in [3, def. 1. 2] Sobolev spaces are defined as bellow.

Definition 2.1 *(Sobolev Space) Let $\Omega \subset \mathbb{R}^d$ be an open set with piecewise smooth boundary, let $m \in \mathbb{N}_{\geq 0}$. Then*

$$H^m(\Omega) := \{v \in L^2(\Omega) |\ D^\alpha v \in L^2(\Omega) \quad \textit{for all} \quad |\alpha| \leq m\}, \tag{2.5a}$$
$$\textit{where} \quad D^\alpha = \frac{\partial^{|\alpha|}}{\partial^{\alpha_1}\partial^{\alpha_2}\cdots\partial^{\alpha_n}} \tag{2.5b}$$
$$\textit{and} \quad |\alpha| = |\alpha_1| + |\alpha_2| + \cdots + |\alpha_n| \quad \textit{for} \quad \alpha \in \mathbb{N}^n. \tag{2.5c}$$

Together with the inner product

$$\langle u, v\rangle_{m;\Omega} := \sum_{|\alpha|\leq m} \langle D^\alpha u, D^\alpha v\rangle_{L^2(\Omega)}, \tag{2.6a}$$

which induces the norm

$$\|u\|_{m;\Omega} := \sqrt{\sum_{|\alpha|\leq m} \|D^\alpha u\|^2_{L^2(\Omega)}} \tag{2.6b}$$

$H^m(\Omega)$ is a Hilbert space [3, chp. 1]. Furthermore, a semi-norm on $H^m(\Omega)$ is given by

$$|u|_{m;\Omega} := \sqrt{\sum_{|\alpha|=m} \|D^\alpha u\|^2_{L^2(\Omega)}}. \tag{2.6c}$$

For reasons of simplicity it is written H^m, $\|\cdot\|_m$ and $|\cdot|_m$, if the domain of definition Ω is avoidable.

Theorem 2.2 *[3, chp. II, § 1, Satz. 1.3, without proof] Let $\Omega \subset \mathbb{R}^d$ be open with piecewise smooth boundary, let $m \in \mathbb{N}_{\geq 0}$. Then $C^\infty(\Omega) \cap H^m(\Omega)$ is dense in $H^m(\Omega)$.*

Hence by the above theorem the completion of the space of smooth functions with respect to the Sobolev norm (2.6b) is the corresponding Sobolev space (2.5a). This result is used in the proof of the existence of the solution to the weak formulation for elliptic BVPs. However, due to the limitation of the scope of this work well-defines is not elaborated in detail an the reader is refereed to the literature, e. g. : [3, chp. II, § 1, Friedriche Ungleichung and Existenz von Lösungen].

Furthermore, the trace theorem gives a Hilbert space, whose dual space contains the restrictions on the boundary of the normal component of the primal variable. The restriction is called trace. But this theorem restricts the domain of definition Ω by the so called *cone condition* for the boundary of the domain.

Definition 2.3 (Cone condition) *[3, chp. II, §1, Theorem 1.9, Rellichscher Auswahlsatz] Let $\Omega \subset \mathbb{R}^d$ be a domain and let the interior angles be positive such that any cone with positive vertical angle can be shifted in Ω such that it meets the corners (see figure 2.2).*

For Ω bounded we have $C^1(\Omega) \subset H^1(\Omega)$, since continuous functions are square integrable.

Theorem 2.4 (Trace Theorem) *[3, chp. II, § 3, 3.1 Spursatz] Let $\Omega \subset \mathbb{R}^d$ be a bounded open set with piecewise smooth boundary Γ, which satisfies the cone condition. There exists a linear bounded map $\gamma : H^1(\Omega) \to L^2(\Gamma)$, such that*

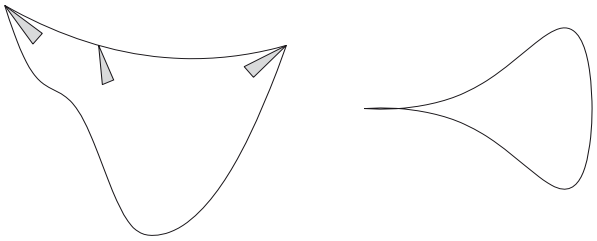

Figure 2.2: Domains satisfying the cone condition (left) and violating. Source: [3, Abb. 6]

i) $\gamma(v) = tr(v)|_\Gamma := v|_\Gamma \quad$ *for all* $\quad v \in C^1(\overline{\Omega})$.

ii) There exists a constant $\quad C > 0 \quad$ *such that* $\quad \|\gamma(v)\|_{0;\Gamma} \leq C\|v\|_{1;\Omega}$.

The image of the above map is called the *trace space* of functions in $H^1(\Omega)$ and $tr(v)|_\Gamma$ is called the trace of v. Moreover, for a Lipschitz-continuous boundary Γ [2, chp. 1.2, p. 5] we have

$$H^{1/2}(\Gamma) := \gamma(H^1(\Omega)) \tag{2.8a}$$

is equipped with the norm [2, eq. 1.2.9]

$$\|g\|_{\frac{1}{2};\Gamma} := \inf_{v \in H^1(\Omega), \gamma(v)=g} \|v\|_{1;\Omega}. \tag{2.8b}$$

The dual space of $H^{1/2}(\Gamma)$ is denoted by $H^{-1/2}(\Gamma)$. The norm on the dual space $H^{-1/2}(\Gamma)$ is given by [2, chp. 1.2]

$$\|v^*\|_{-\frac{1}{2};\Gamma} := \sup_{v \in H^{1/2}(\Gamma)} \frac{\langle v, v^* \rangle}{\|v\|_{\frac{1}{2};\Gamma}}. \tag{2.8c}$$

Due to the scope of this work the above Sobolev spaces of fractional order are not discussed.
In this work it is defined as in [3, chp. II, § 1, Def. 1.4] that

Definition 2.5 *$H_0^m(\Omega)$ is the closure of $C_0^\infty(\Omega)$ with respect to the Sobolev norm $\|\cdot\|_{m;\Omega}$.*

The Poincaré inequality [2, eq. 1.2.14], which holds for all Ω as above, is given by

$$\begin{aligned} &\|v\|_{0;\Omega} \leq C(\Omega)|v|_{1;\Omega} \quad \text{for all} \quad v \quad \text{in} \quad H_0^1(\Omega), \\ &\quad \text{for some} \quad C(\Omega) > 0. \end{aligned} \tag{2.9}$$

This inequality is used in order to show the existence of a solution to weak problems of the form given in definition 2.8 [3, chp. II , § 2, Aufg. 2.10, proof theorem 2.9 Existenzsatz], which will be introduced in this work (eq.

(2.22a)) .
Furthermore, as in [2, eq. 1.2.15], it is defined for $\Gamma_D \subseteq \partial\Omega$

$$H^1_{0;\Gamma_D}(\Omega) := \{v \in H^1(\Omega) |\ v\big|_{\Gamma_D} = 0\}. \tag{2.10a}$$

Finally in the search space of solutions for the saddle point problem (2.2.2) the space

$$H(div;\Omega) = \{\mathbf{q} \in \left(H^0(\Omega)\right)^d |\ \mathrm{div}(\mathbf{q}) \in H^0(\Omega)\} \tag{2.11a}$$

with the norm [2, eq. 2.1.15]

$$\|q\|_{\mathrm{div};\Omega} := \sqrt{|\mathbf{q}|^2_{0;\Omega} + |\mathrm{div}(\mathbf{q})|^2_{0;\Omega}}, \tag{2.11b}$$

occurs. Green's formula is applicable in $H(div;\Omega)$ as stated in the following.

Lemma 2.6 *[2, lemma 2.1.1]. For* $\mathbf{q} \in H(div;\Omega)$*, we can define* $\mathbf{q}\cdot\mathbf{n}\big|_\Gamma \in H^{-1/2}(\Gamma)$ *and we have Green's formula,*

$$\int_\Omega div(\mathbf{q}) v\, d\mathbf{x} + \int_\Omega \mathbf{q}\cdot\nabla v\, d\mathbf{x} = \langle \mathbf{q}\cdot\mathbf{n}, v\rangle := \int_\Gamma \mathbf{q} v\cdot\mathbf{n}\, d\sigma(\mathbf{x}) \quad \textit{for all} \quad v \in H^1(\Omega). \tag{2.12}$$

Proof A proof can be found in [2]. □

By the above lemma the trace of the normal component of functions in $H(div;\Omega)$ are elements of $H^{-1/2}(\Gamma)$ and it turns out that the image of the trace operator is the dual space $H^{-1/2}(\Gamma)$ as stated below.
$\langle\cdot,\cdot\rangle$ is called duality pairing between $H^{-\frac{1}{2}}(\Gamma)$ and $H^{\frac{1}{2}}(\Gamma)$ [2, chp. 1.2].

Lemma 2.7 *[2, lemma 2.1.2] The trace operator* $\gamma : \mathbf{q} \in H(div;\Omega) \to \mathbf{q}\cdot\mathbf{n}\big|_\Gamma \in H^{-1/2}(\Gamma)$ *is surjective.*

2.2.2 Weak Formulation and Saddle Point Problem

The problem, which is sought to be solved, using numerical methods, the saddle point problem, is also known as weak formulation of the continuous problem. In the following the weak solution formulation to the continuous problem (2.1) is introduced.

Weak solutions This section follows the approach in [11, chp. 4 Schwache Lösungen].
Let $\Omega \subset \mathbb{R}^d, d \geq 2$ be a bounded open domain with Lipschitz boundary $\Gamma = \partial\Omega$, which implies the cone condition is satisfied. Assume $u \in C^2(\Omega)$

is a solution of (2.1). Let $v \in C_0^\infty(\Omega)$. By multiplying (2.1a) with v and integrating over Ω it follows that

$$\int_\Omega -\operatorname{div}(A\nabla u)v + buv \, d\mathbf{x} = \int_\Omega fv \, d\mathbf{x}. \tag{2.13}$$

Note that the above integral is well defined since Ω is bounded and by the smoothness assumptions on u and v. Using Green's formula it is obtained that

$$\int_\Omega A\nabla u \cdot \nabla v + buv \, d\mathbf{x} - \int_\Gamma A\nabla uv \cdot \mathbf{n} \, d\sigma(\mathbf{x}) = \int_\Omega fv \, d\mathbf{x}, \tag{2.14}$$

where $\mathbf{n}$ denotes the outwards pointing unit normal vector on Γ. Since u vanishes on the boundary Γ it follows that

$$\int_\Omega A\nabla u \cdot \nabla v + buv \, d\mathbf{x} = \int_\Omega fv \, d\mathbf{x}. \tag{2.15}$$

Recall that $C_0^\infty(\Omega)$ is dense in $H_0^1(\Omega)$ by definition 2.5 and therefore

$$\int_\Omega A\nabla u \cdot \nabla v + buv \, d\mathbf{x} = \int_\Omega fv \, d\mathbf{x} \quad \text{for all} \quad v \in H_0^1(\Omega). \tag{2.16}$$

Moreover, for the mixed Neumann problem, that writes as for $\Gamma_D \subset \partial\Omega$

$$Lu = f \quad \text{on} \quad \Omega \tag{2.17a}$$
$$\mathbf{n} \cdot \nabla u = g \quad \text{on} \quad \partial\Omega \setminus \Gamma_D \quad \text{and} \tag{2.17b}$$
$$u = 0 \quad \text{on} \quad \Gamma_D, \tag{2.17c}$$

a similar proceeder can be applied, which motivates to define:

Definition 2.8 (Weak solution) *[3, chp. II, § 2, def. 2.8] Let for $u, v \in H_0^1(\Omega)$, respectivly $u, v \in H_{0;\Gamma_D}^1(\Omega)$ be the symmetric bilinear form $a(\cdot,\cdot)$ be given by*

$$a(u,v) := \int_\Omega A\nabla u \cdot \nabla v + buv \, d\mathbf{x}. \tag{2.18}$$

i) A function $u \in H_0^1(\Omega)$ is called weak solution of the elliptic boundary value problem (2.1) with a homogeneous Dirichlet BC if

$$a(u,v) = \langle f, v\rangle_{0;\Omega} \quad \textit{for all} \quad v \in H_0^1(\Omega). \tag{2.19a}$$

ii) A function $u \in H_{0;\Gamma_D}^1(\Omega)$ is called weak solution of the elliptic boundary value problem (2.17) with mixed Neumann BC if

$$a(u,v) = \langle f, v\rangle_{0;\Omega} + \langle A^{-1}g, v\rangle \quad \textit{for all} \quad v \in H_{0;\Gamma_D}^1(\Omega). \tag{2.19b}$$

Note that it is straight forward to show that any classical solution $u \in C^2(\Omega)$ of (2.1) or (2.17) is a weak solution.

We have defined $H(\operatorname{div},\Omega)$, $H^0(\Omega)$ and $H_{0;\Gamma}^1(\Omega)$. Since the focus of this work is implementation, weak solutions and bilinear forms are not studied in detail. Thus the saddel point problem is defined:

Statement of the Saddle Point Problem [15, eq. 2] Find $(\mathbf{j_p}, u_p, u_d) \in H(\mathrm{div};\Omega_p) \times H^0(\Omega_p) \times H^1_{0;\Gamma_d}(\Omega_d)$ such that

$$\begin{aligned} a_1(\mathbf{j}_p, \mathbf{q}_p) + b(\mathbf{q}_p, u_p) \quad & -d(\mathbf{q}_p, u_d) = 0 \\ & \text{for all} \quad \mathbf{q}_p \in H(\mathrm{div};\Omega_p), && \text{(2.20a)} \\ b(\mathbf{j}_p, v_p) - c(u_p, v_p) \quad & = -\langle f, v_p\rangle_{0;\Omega_p} \\ & \text{for all} \quad v_p \in H^0(\Omega_p) \quad \text{and} && \text{(2.20b)} \\ -d(\mathbf{j}_p, v_d) \quad & -a_2(u_d, v_d) = -\langle f, v_d\rangle_{0;\Omega_d} \\ & \text{for all} \quad v_d \in H^1_{0;\Gamma_d}(\Omega_d), && \text{(2.20c)} \end{aligned}$$

where the bilinear forms $a_1(\cdot,\cdot)$, $a_2(\cdot,\cdot)$, $b(\cdot,\cdot)$, $c(\cdot,\cdot)$ and $d(\cdot,\cdot)$ are given by

$$\begin{aligned} a_1(\mathbf{p}_p, \mathbf{q}_p) &:= \int_{\Omega_p} A^{-1}\mathbf{p}_p \cdot \mathbf{q}_p \, d\mathbf{x} \\ &\quad \text{for all} \quad \mathbf{p}_p, \mathbf{q}_p \in H(\mathrm{div};\Omega_p), && \text{(2.21a)} \\ a_2(w_d, v_d) &:= \int_{\Omega_d} A\nabla v_d \nabla w_d + b v_d w_d \, d\mathbf{x} \\ &\quad \text{for all} \quad v_d, w_d \in H^1_{0;\Gamma_d}(\Omega_d), && \text{(2.21b)} \\ b(\mathbf{q}_p, v_p) &:= \int_{\Omega_p} \mathrm{div}(\mathbf{q}_p) v_p \, d\mathbf{x} \\ &\quad \text{for all} \quad v_p \in H^0(\Omega_p), \mathbf{q}_p \in H(\mathrm{div};\Omega_p), && \text{(2.21c)} \\ c(w_p, v_p) &:= \int_{\Omega_p} b w_p v_p \, d\mathbf{x} \\ &\quad \text{for all} \quad v_p, v_d \in H^0(\Omega_p) \quad \text{and} && \text{(2.21d)} \\ d(\mathbf{q}_p, v_d) &:= \langle \mathbf{q}_p \cdot \mathbf{n}, v_d\rangle, \\ &\quad \text{for all} \quad \mathbf{q}_p \in H(\mathrm{div};\Omega_p), v_d \in H^1_{0,\Gamma_d}(\Omega_d). && \text{(2.21e)} \end{aligned}$$

This problem can be shown to have a unique solution as written in [15].

2.3 Model Problem

In this work the Poisson's problem [2, eq. 1.2.22], which is

$$-\Delta u = f \quad \text{in} \quad \Omega \tag{2.22a}$$

with a Dirichlet boundary condition

$$u = 0 \quad \text{on} \quad \partial\Omega, \tag{2.22b}$$

is investigated.

2.3.1 Poission's Equation as Saddle Point Problem

The weak formulation of the problem (2.1) restricted to the above special case (2.22), since A is the identity and $b = 0$, writes as:
Find $(\mathbf{j}_p, u_p, u_d) \in H(\mathrm{div}; \Omega_p) \times H^0(\Omega_p) \times H^1_{0;\Gamma_d}(\Omega_d)$, such that

$$
\begin{aligned}
a_1(\mathbf{j}_p, \mathbf{q}_p) + b(\mathbf{q}_p, u_d) \qquad & -d(\mathbf{q}_p, u_d) = 0 && \text{(2.23a)}\\
& \qquad \text{for all} \quad \mathbf{q}_p \in H(\mathrm{div}; \Omega_p), \\
b(\mathbf{j}_p, v_p) \qquad & = -\langle f, v_p \rangle_{0;\Omega_p} && \text{(2.23b)}\\
& \qquad \text{for all} \quad v_p \in H^0(\Omega_p) \quad \text{and} \\
-d(\mathbf{j}_p, v_d) \qquad & -a_2(u_d, v_d) = -\langle f, v_d \rangle_{0;\Omega_d} && \text{(2.23c)}\\
& \qquad \text{for all} \quad v_d \in H^1_{0;\Gamma_d}(\Omega_d).
\end{aligned}
$$

A formulation of the above variational problem as weak problem, using integrals, can be found in appendix A.1.

Chapter 3

Discretization

In this work the variational problem (2.23) is sought to be solved using the method of finite element. In this method the domain Ω is divided into a finite number of sub domains, these are called the elements. Moreover on every element a polynomial is obtained. This chapter introduces the concept of finite elements.

The first text book about finite elements had been published in 1967 (Zienkiewicz, O.C. and Cheung, Y.K, The Finite Element Method in Structural and Continuum Mechanics, McGraw-Hill, London) [10]. The method was developed by engineers, who used polynomials in oder to solve variational problems [17]. Even though, then it had been named finite difference method (Zlámal, 1968 [17]) it is an alternative to finite differences (Strang, 1971 [13]). Finite differences use difference quotients for approximating a differential equation [13]. Due to the flexibility in the geometry finite elements were called superior to finite differences [13]. Today finite element methods are a universal tool in solid mechanics [16], fluid dynamics [8] or electromagnetism [12].

A partition of the bounded domain $\Omega \subset \mathbb{R}^2$ into a finite set of polygons $\mathcal{K}$ is used. In the case of triangles, it is written $\mathcal{T}$ for the *triangulation* [2, chp. 7]. Due to the limitation of the scope of this work the reader is referred to the literature like [2, chp. 2.2, chp. 7.1.4] for details. In the case of rectangles it is written $\mathcal{R}$ and they are called two-dimensional *bilinear* rectangular elements [11, chp. 6] and the partition is called *rectangulation*.

3.1 Finite Elements

Definition 3.1 *[3, chp. II, §5, Def. 5.8][2, chp. 2.2.1] A finite element (FEM) is a triple* (K, Π, Σ) *with the following properties:*

(i) K *is a polyhedron in* $\mathbb{R}^d$*. (The parts of the surface* ∂K *lie on a hyperplane and are called faces.)*

(ii) Π *is a subspace of* $C(K)$ *of finite dimension* s*. (Functions in* Π *are called shape functions if they are a basis of* Π*.* s *is called the number of local degrees of freedom).*

(iii) Σ *is a set of* s *linearly independent functionals in* Π*. Every* $p \in \Pi$ *is uniquely defined by the values of the* s *functionals in* Σ*. (These linear forms* $\{l_i\}_{1 \le i \le s}$ *are called local degrees of freedoms.)*

The following notations and abbreviations are used:

- It is written $\mathcal{K}_h$ instead of $\mathcal{K}$, if every element $K \in \mathcal{K}_h$ has a diameter smaller or equal to h.
- $\hat{K}$ denotes the reference element. The change of variables for $K \in \mathcal{K}$ is given by $F : \hat{K} \to K$ and for p a polynomial on K, $p|_K = \hat{p} \circ F^{-1}$, where $\hat{p} : \hat{K} \mapsto \mathbb{R}$.
- $\hat{P}$ denotes a set of polynomials on $\hat{K}$.
- $\hat{\Sigma}$ denotes a set of degrees of freedom on $\hat{P}$ that is, a set of linear forms $\{\hat{l}_i\}_{1 \le i \le \dim \hat{P}}$ on $\hat{P}$.

Definition 3.2 *[3, see chp. II, §5, p. 57] A family of finite elements* $S = \{(K_j, \Pi_j, \Sigma_j)\}_{K_j \in \mathcal{K}}$ *is called conforming if the associated function space* $S(\Omega; \mathcal{K})$ *is contained in the space* $H(\Omega)$*, in which the variational problem is formulated.*

Definition 3.3 *[3, chp. II, §5, def. 5.12] A family of finite elements* S *for a partition* $\mathcal{K}$ *of* $\Omega \subset \mathbb{R}^d$ *is called an affine family provided there exists a finite element* $(\hat{K}, \hat{\Pi}, \hat{\Sigma})$ *called the reference element with the following properties: For every* $K_j \in \mathcal{K}$*, there exists an affine mapping* $F_j : \hat{K} \mapsto K_j$ *such that for every* $v \in S(\Omega, \mathcal{K})$*, its restriction to* K_j *has the form*

$$v(x) = \hat{p}(F_j^{-1}(x)) \quad \textit{for some} \quad \hat{p} \in \hat{P}. \tag{3.1}$$

Lemma 3.4 *[2, chp. 2.2.2, lem. 2.2.3] Let* K *be an affine element of dimension* k *with vertices* $\mathbf{x}_i, 1 \le i \le k$*. There exists a set* $\{\lambda_i(\mathbf{x})\}_{1 \le i \le k}$ *of linear functions on* K*, called barycentric coordinates, satisfying*

$$\lambda_i(\mathbf{x}_j) = \delta_{i,j} \quad \textit{and} \quad \sum_{i=1}^{k} \lambda_i(\mathbf{x}) = 1 \quad \textit{for all} \quad \mathbf{x} \in K. \tag{3.2}$$

$\delta_{i,j}$ denotes the Kronecker delta.

Definition 3.5 *[2, chp. 2.2.1, eq. 2.2.8] A finite element (K, Π, Σ) is of Lagrange type if its degrees of freedoms are point values, that is, if one is given a set $\{\hat{\mathbf{y}}_i\}_{1 \le i \le dim(\hat{P})}$ of points in $\hat{K}$ and one defines*

$$\hat{l}_i(\hat{p}) = \hat{p}(\hat{\mathbf{y}}_i), \quad 1 \le i \le dim(\hat{P}). \tag{3.3}$$

3.2 Polynomial Spaces

In the following the two dimensional case, $d = 2$, is considered. This section defines scalar valued polynomial spaces.

For triangular elements T the space of polynomials of degree less or equal to k on T in is denoted by

$$P_k(T) := \{p : T \to \mathbb{R} |\ p(\mathbf{x}) = \sum_{0 \le i,j;\ i+j \le k} a_{i,j}(x^1)^i (x^2)^j\} \tag{3.4}$$

Note that $\dim(P_k(T)) = \frac{1}{2}(k+1)(k+2)$ [2, chp. 2.2.1].

For rectangular elements R as in [2, chp. 2.2.1] the space of polynomials on the elements is given by

$$P_k(R) := \{p : R \to \mathbb{R} |\ p(\mathbf{x}) = \sum_{i,j=0}^{k} a_{i,j}(x^1)^i (x^2)^j\}. \tag{3.5}$$

Note that $\dim(P_k(R)) = 2(k+1)(k+1)$ [2, chp. 2.2.1].
The space of square integrable functions on the boundary of R, which are polynomials of degree less or equal to k on each edge e_i of R, is denoted by

$$R_k(\partial R) := \{\varphi \in H^0(\partial R) |\ \varphi\big|_{e_i} \in P_k(e_i)\ \forall e_i\}, \tag{3.6}$$

like in [2, chp. 2.2.1]. Note that $\dim(R_k(\partial R)) = 4(k+1)$ [2, chp. 2.2.1].

For a partition $\mathcal{K}$ of Ω, let $S_k(K)$ be a subspace of $P_k(K)$ for all $K \in \mathcal{K}$ and define

$$\mathcal{L}^s(S_k, \mathcal{K}) := \{v \in H^s(\Omega) |\ v\big|_K \in S_k(K)\ \forall K \in \mathcal{K}\}. \tag{3.7}$$

Note that $\mathcal{L}^s(S_k, \mathcal{K}) \subset C^{s-1}(\overline{\Omega})$, it is build up of piecewise polynomials, although $H^s \not\subseteq C^{s-1}(\overline{\Omega})$ [2, chp. 2.2.3, rmk. 2.2.3]. For approximating $H^1(\Omega)$ Lagrange type elements are sufficient [2, chp. 2.2.1]. Whereas the choice of points as in figure 3.1 is determined by whether degrees of freedom are linearly independent [2, chp. 2.2.2, rmk. 2.2.2].
E. g. for the weak problem associated with the Dirichlet problem (2.19) a FEM family S is called conforming if $S(\Omega; \mathcal{K}) \subset H_0^1(\Omega)$. $S(\Omega, \mathcal{K})$ is called FEM-space in the following.

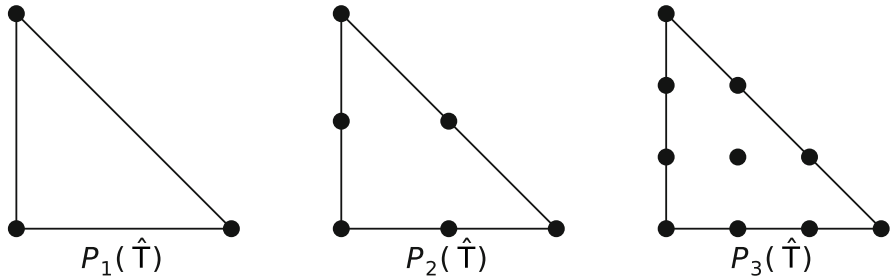

Figure 3.1: Triangular conforming elements and nodes associated to degrees of freedom, source: [2, fig. 2.3]

3.2.1 Approximation of $H^1_{0;\Gamma}(\Omega)$

Similarly as in [11, chp. 7], we defined for $\mathcal{T}$ a triangulation of Ω and $\Gamma \subseteq \partial\Omega$,

$$S^k(\Omega, \mathcal{T}) := \{\varphi \in H^0(\Omega) |\ \varphi|_T \in P_k(T) \forall T \in \mathcal{T}\} \cap C^0(\Omega) \quad \text{and} \tag{3.8a}$$

$$S^k_{0;\Gamma}(\Omega, \mathcal{T}) := \{p \in S^k(\Omega, \mathcal{T}) |\ \varphi|_\Gamma = 0\}. \tag{3.8b}$$

3.2.2 Approximation of $H^0(\Omega)$

As in [15] the space of square integrable functions on Ω, which are polynomials on the elements of a rectangulation $\mathcal{R}$ of Ω, is denoted by

$$W_k(\Omega; \mathcal{R}) := \{v \in H^0(\Omega) |\ v\big|_R \in P_k(R), R \in \mathcal{R}_h\}. \tag{3.9}$$

3.3 Approximation of $H(\mathbf{div}; \Omega)$

The aim of this section is to define a search space for a function in $H(\mathrm{div}; \Omega)$. Let R be a rectangle and e_i, $1 \leq i \leq 4$ denote the faces of R.
Piecewise polynomial vectors on R are given by

$$\mathbf{P}_k(R) := \big(P_k(R)\big)^2. \tag{3.10}$$

Furthermore, we define

$$\mathbf{P}^s_{\mathbf{k}+\mathbf{x}k}(R) := \{\mathbf{p} \in \big(\mathbf{P}_k(R) + \mathbf{x}P_k(R)\big) |\ \mathbf{p} \cdot \mathbf{n} \in R_s(\partial R)\}. \tag{3.11}$$

These spaces contain piecewise polynomials vectors on R with polynomial and square integrable normal component of degree at most s on the boundary of R [2, ch. 2.3.1].
The *local Raviart-Thomas space* of order k is given by [2, eq. 2.4.1]

$$\mathcal{RT}_k(R) := \mathbf{P}^k_{\mathbf{k}+\mathbf{x}k}(R). \tag{3.12}$$

Note that elements of $\mathcal{RT}_k(R)$ are of the form $\mathbf{p}(\mathbf{x}) + \mathbf{x}q(\mathbf{x})$, where $\mathbf{p} \in \mathbf{P}_k(R)$ and $q(\mathbf{x}) \in P_k(R)$.

Since for $\mathbf{q} \in \mathbf{P}_k^s(R)$ it follows that $\mathrm{div}(\mathbf{q}) \in P_{k-1}(R)$ and the normal component of the trace, $\mathbf{q} \cdot \mathbf{n}|_{\partial R}, \in R_s(\partial R)$. Therefore, finding a suitable set of degrees of freedom built $\mathbf{P}_k^s$ is dependent on finding a continuity assumption of $\mathbf{q} \cdot \mathbf{n}$ at the interfaces of edges [2, chp. 2.3.1].
In the following the so called conforming *lowest order Raviart-Thomas space*

$$\mathcal{RT}_0(\Omega, \mathcal{R}) = \{\mathbf{q} \in H(\mathrm{div}, \Omega) |\ \mathbf{q}|_R \in \mathcal{RT}_0(R) \forall R \in \mathcal{R}\} \tag{3.13}$$

is considered. However $\mathcal{RT}_0(R)$ is a four dimensional space [2, chp. 2.4.1, eq. 2.4.1] and therefore on each rectangle four functions in $\mathcal{RT}_0(R)$ can be specified by the four normal components of $\mathbf{q}$ on ∂R, which are illustrated in figure 3.2.

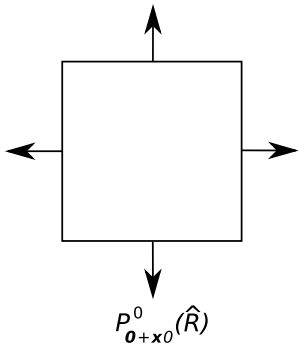

Figure 3.2: Four normal components of $\mathbf{q} \in \mathcal{RT}_0(\hat{R})$ on $\partial\hat{R}$, adapted from [2, fig. 2.16]

3.4 Galerkin Discretized Problem

A Rayleigh-Ritz-Galerkin discretization method, is used whenever an imposed method solves a given problem on a finite dimensional subspace of the search space (here $\mathcal{RT}_0, W_0$ and $S^1_{0;\Gamma_d}$) [11, chp. 7], [14, chp. 2].

The saddle point problem (2.23) is discretized similarly as in [15, eq. 3]. It writes as:

Find $(\mathbf{j}_{h_p}, u_{h_p}, u_{h_d}) \in \mathcal{RT}_0(\Omega_p; \mathcal{R}_{h_p}) \times W_0(\Omega_p; \mathcal{R}_{h_p}) \times S^1_{0;\Gamma_d}(\Omega_d; \mathcal{T}_{h_d})$ such that

$$
\begin{aligned}
a_1(\mathbf{j}_{h_p}, \mathbf{q}_{h_p}) + b(\mathbf{q}_{h_p}, u_{h_p}) \quad & -d(\mathbf{q}_{h_p}, u_{h_d}) = 0 && \text{(3.14a)}\\
& \text{for all} \quad \mathbf{q}_{h_p} \in \mathcal{RT}_0(\Omega_p; \mathcal{R}_{h_p}),\\
b(\mathbf{j}_{h_p}, w_{h_p}) \quad & = -\langle f, w_{h_p}\rangle_{0;\Omega_p} && \text{(3.14b)}\\
& \text{for all} \quad w_{h_p} \in W_0(\Omega_p; \mathcal{R}_{h_p}),\\
-d(\mathbf{j}_{h_p}, v_{h_d}) \quad & -a_2(u_{h_d}, v_{h_d}) = -\langle f, v_{h_d}\rangle_{0;\Omega_d} && \text{(3.14c)}\\
& \text{for all} \quad v_{h_d} \in S^1_{0;\Gamma_d}(\Omega_d; \mathcal{T}_{h_d}).
\end{aligned}
$$

Due to the limitation of the scope of this work convergence is not elaborated. But convergence of a mixed conforming FEM as introduced, has been proven in [15]. For two triangular discretizations, $\mathcal{T}_{h_p}$ and $\mathcal{T}_{h_d}$, the following a priori error estimate for the discretization error can be show:

Lemma 3.6 *For $(\mathbf{j}, u)$ the solution of (2.23) the discretized solution $(\mathbf{j}_{h_p}, u_{h_p}, u_{h_d}) \in \mathcal{RT}_0(\Omega_p, \mathcal{T}_{h_p}) \times W_0(\Omega_p, \mathcal{T}_{h_p}) \times S^1_{0;\Gamma_d}(\Omega_d, \mathcal{T}_{h_d})$ of above (3.14) satisfies (if the problem has a regular enough solution)*

$$
\begin{aligned}
\|\mathbf{j} - \mathbf{j}_{h_p}\|^2_{div;\Omega_p} + \|u - u_{h_p}\|^2_{0;\Omega_p} + \|u - u_{h_d}\|^2_{1;\Omega_d}&\\
\leq C\big(h_p^2(\|u\|^2_{1;\Omega_p} + \|\mathbf{j}\|^2_{1;\Omega_p} + \|f\|^2_{1;\Omega_p}) + h_d^2\|u\|^2_{2;\Omega_d}\big) \quad &\text{(3.15)}
\end{aligned}
$$

Remark 3.7 *[15] The constant C in eq. (3.15) is independent of the ratio of h_p and h_d and no matching condition for the triangulations $\mathcal{T}_{h_p}$ and $\mathcal{T}_{h_d}$ at the interface is required.*

3.5 Triangular conforming Linear Finite Elements

In the following section the basis used in the MATLAB implementation for conforming *linear FEM* is introduced. In particular the shape functions of the FEM triplet $(K, \Pi, \Sigma) = (T, P_1(T), \{l_{T,x_i}\}_{1\leq i\leq 3})$ and the continuity condition are stated, which induces conforming elements.

Let $\mathcal{T}$ be a family of triangular elements. For $S = P_k(\mathcal{T})$ any FEM is affine [3, chp. II, §5, Bem. 5.3], because polynomials transform to polynomials under affine linear transformations. It suffice to derive a local basis, a basis defined on the reference element $\hat{T}$, in order to determine a basis of $P_k(\mathcal{T})$. In particular the local basis is transformed to an arbitrary element T.
The reference element is defined as $\hat{T} = \text{conv}\{(0,0)^\intercal, (1,0)^\intercal, (0,1)^\intercal\}$ as in LehrFEM [4, chp. 2, p. 23].

Remark 3.8 *[3, II, §5, Bem. 5.4] Let $T = conv\{\mathbf{x}_1, \mathbf{x}_2, \mathbf{x}_3\} \in \mathcal{T}$. There exists exactly one $p \in P_1(T)$, which solves the interpolation problem $p(\mathbf{x}_i) = f(\mathbf{x}_i)$ for $i = 1, 2, 3$, for some given $f : \mathbb{R}^2 \to \mathbb{R}$.*

Proof A more general form of the above remark is proven in [3]. It uses that due to (3.2) $\dim(P_1(\hat{T})) = 3$ and affinity. □

Lemma 3.9 *[11, chp. 7], [2, chp. 2.2.2] For $T = conv\{\mathbf{x}_1, \mathbf{x}_2, \mathbf{x}_3\} \in \mathcal{T}$ barycentric coordinates,*

$$\lambda_{T,x_i}(\mathbf{x}) := \frac{det(\mathbf{x}_{i+1}^\top - \mathbf{x}^\top, \mathbf{x}_{i-1}^\top - \mathbf{x}_{i+1}^\top)}{det(\mathbf{x}_{i+1}^\top - \mathbf{x}_i^\top, \mathbf{x}_{i-1}^\top - \mathbf{x}_{i+1}^\top)} = \frac{|T_{x,x_{i+1},x_{i-1}}|}{|T|}, \quad for \quad 1 \leq i, j \leq 3, \quad (3.16)$$

where $T_{x,x_{i+1},x_{i-1}} = conv\{\mathbf{x}, \mathbf{x}_{i+1}, \mathbf{x}_{i-1}\}$ and the above indices are modulo 3, are shape functions of $P_1(T)$. Furthermore let $l_{T,x_i} : P_1(T) \to \mathbb{R}$, be given by

$$l_{T,x_i}(p) := p(\mathbf{x}_i) \quad for \quad 1 \leq i \leq 3. \quad (3.17)$$

Then $(T, P_1(T), \{l_{T,x_i}\}_{1 \leq i \leq 3})$ is of Lagrangian type.

Proof Recall it suffice to show that $\{\lambda_{T,x_i}\}$ is a linearly independent subset of $P_1(T)$ and that every element in $P_1(T)$ is uniquely defined by the three values $\hat{l}_{\hat{T},\hat{x}_i}$. The first part is shown in [11, chp. 7] and the second part follows directly form remark 3.8 and the affinity. □

Similarly as in [11, chp. 7] the *node basis* of $\mathcal{L}^1(P_1(T), \mathcal{T})$ is defined.

Definition 3.10 (Hat functions) *Let $\mathcal{T}$ be a triangulation of $\Omega \subset \mathbb{R}^2$, a polygonal bounded domain. Then $\mathcal{T} = (\Theta, \mathcal{E})$ is a graph, where the nodes and edges are given by*

i) $\Theta := \{$ *the set of vertecies of all triangles in* $\mathcal{T}\}$,

ii) $\mathcal{E} := \{$*the set of all edegs of triangles in* $\mathcal{T}\}$ *and*

iii) for all $\mathbf{x}_i \in \Theta$, $\omega_i := \bigcup_{T \in \mathcal{T},\ \mathbf{x}_i \in \overline{T}} T$, *is called a patch.*

Then the hat functions on $\mathcal{T}$ are given by

$$b_{x_k}(\mathbf{x}) := \begin{cases} \lambda_{T,i}(\mathbf{x}) & if \quad \mathbf{x} \in T \subset \omega_k \quad and \quad \mathbf{x}_i = \mathbf{x}_k, \\ 0 & if \quad \mathbf{x} \notin \omega_i. \end{cases} \quad (3.18)$$

Note that a patch ω_i is a subset of $\mathcal{T}$, where all elements share one vertex $\mathbf{x}_i$ [4, chp. 1].

Lemma 3.11 *Let b_{x_k} be given as above. Then for all $\mathbf{x}_k \in \Theta$*

i) $b_{x_k} \in C^0(\overline{\Omega})$,

ii) $b_{x_k} \in P_1(T)$ *for all* $T \in \mathcal{T}$ *and*

iii) $b_{x_k}(\mathbf{x}_i) = \delta_{k,i}$ *for all* $\mathbf{x}_i \in \Theta$.

Proof For $\mathbf{x}_k \in \Theta$ assume b_{x_k} is given as in (3.18) then,

i) $b_{x_k}(\mathbf{x})|_{\partial\omega_k} = 0$ and therefore it is continuous.

ii) and iii) follow directly from lemma 3.9. □

Since a Dirichlet boundary condition as in (2.22a) must be satisfied by any conforming FEM space in $H^1_{0;\Gamma}(\Omega)$, roughly speaking, the hat functions are equipped with a boundary condition.

Definition 3.12 *[11, chp. 7] Let $\mathcal{T} = (\Theta, \mathcal{E})$ be a triangularization of Ω a polygonal domain and $\Gamma_D \subseteq \partial\Omega$.*

i) The set of interior vertices of Θ are given by

$$\Theta^\circ := \Theta \setminus \{\Theta \cap \Gamma_D\}. \tag{3.19a}$$

ii) The interior hat functions are

$$b^\circ_{x_k}(\mathbf{x}) := \begin{cases} \textit{as given in} \quad (3.18) & \textit{if} \quad \mathbf{x}_k \in \Theta^\circ, \\ 0 & \textit{if} \quad \mathbf{x}_k \in \Theta \setminus \Theta^\circ. \end{cases} \tag{3.19b}$$

Lemma 3.13 *[11, chp. 7] $\{b^\circ_{\mathbf{x}_k}\}_{\mathbf{x}_k \in \Theta}$ is a basis of $S^1_{0;\Gamma_D}(\Omega, \mathcal{T}_h)$.*

Proof A proof can be found in [11]. □

So far a basis, which can be used in the implementation of the FEM method of the dual part of the problem (3.14) was constructed. Using eq. (3.16) it can be concluded that this basis can be easily implemented. Next the basis for discretizing the primal problem is explored.

3.6 Piecewise Constant Finite Elements

Let $\mathcal{R}$ be a regulation of Ω, a rectangular domain. Recall $W_0(\Omega, \mathcal{R})$ is the space of piecewise constant functions on $\mathcal{R}$ (see eq. (3.9)).

Lemma 3.14 *Let $R_j \in \mathcal{R}$ be a rectangular element, let*

$$b_{R_j}(\mathbf{x}) := \begin{cases} 1 & \textit{if} \quad \mathbf{x} \in R_j, \\ 0 & \textit{if} \quad \mathbf{x} \in \partial\Omega \setminus R_j, \end{cases} \tag{3.20}$$

then $\{b_{R_j}\}_{R_j \in \mathcal{R}}$ is a basis of $W_0(\Omega, \mathcal{R})$. This basis is called standard basis of $W_0(\Omega, \mathcal{R})$.

Proof The proof of this lemma is trivial. □

Because one degree of freedom is defined per element, the associated node is chosen as the midpoint of each rectangle, which is illustrated in figure 3.3. The FEM triplet of this space is $(R, P_0(R), l_R)$, where the functional l_R can be defined by $l_R(p) = p(\mathbf{z})$, $p \in P_0(R)$, where $\mathbf{z}$ is the midpoint of R. It follows:

Proposition 3.15 *For R a rectangle, l_R as above $(R, P_0(R), l_R)$ is of Lagrangian type.*

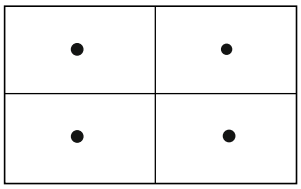

Figure 3.3: Standard constant bilinear elements and associated nodes with degrees of freedom

3.7 Bilinear conforming Raviart-Thomas Finite Elements

Due to details of the implementation in the following the graph given by a regtangulation $\mathcal{R} = (\Theta, \mathcal{E})$ of the domain of definition Ω is an oriented graph, i. e. , every edge $e = \overrightarrow{(\mathbf{x}_A, \mathbf{x}_B)} \in \mathcal{E}$, $\mathbf{x}_A, \mathbf{x}_B \in \Theta$ has a non negligible direction. An oriented rectangulation is illustrated in figure 3.4.

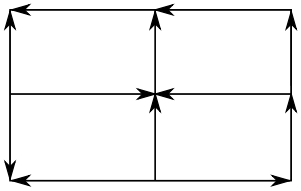

Figure 3.4: Oriented rectentulation $\mathcal{R}$

As justified in section 3.5 also for $S = \mathbf{P}^k_{\mathbf{k}+\mathbf{x}k}(R)$, $R \in \mathcal{R}$ we have affine FEM. But applying the transformation of variable formula to bilinear conforming Raviart-Thomas FEM is not as applicable. In particular $p|_R = \hat{p}(F^{-1})$ if and only if the normal vectors on $\partial\hat{R}$ and their images on ∂R have the same orientation. Hence we first define the support of the basis elements of $\mathcal{RT}_0(\Omega, \mathcal{R})$, second the local function, aiming continuity on the boundary of elements. Note that for $R \in \mathcal{R}$

$$\mathcal{RT}_0(R) = (R, \mathbf{P}^0_{\mathbf{0}+\mathbf{x}0}(R), \{l_{R,p}\}_{1\leq p\leq 4}), \tag{3.21}$$

where $l_{R,p} : \mathbf{P}^0_{\mathbf{0}+\mathbf{x}0}(R) \to \mathbb{R}$ can be defined by $l_{R,p}(\mathbf{q}) = \mathbf{q}(\mathbf{y}_p) \cdot \mathbf{n}_p$, for $\mathbf{y}_p$ the midpoint of an edge e_p of R and $\mathbf{n}_p$ the normal vector on e_p , $1 \leq p \leq 4$ as in [3, chp. III, §5, Das Raviart-Thomas-Element] for triangles. Since $\mathbf{P}^0_{\mathbf{0}+\mathbf{x}0}$ is vector valued, the Raviart-Thomas FEMs are not of Lagrangian type. Therefore we associate edges to the degrees of freedom.
In the following the reference rectangle $\hat{R}$ is given by $[0,1]^2 \subset \mathbb{R}^2$ as in LehrFEM.

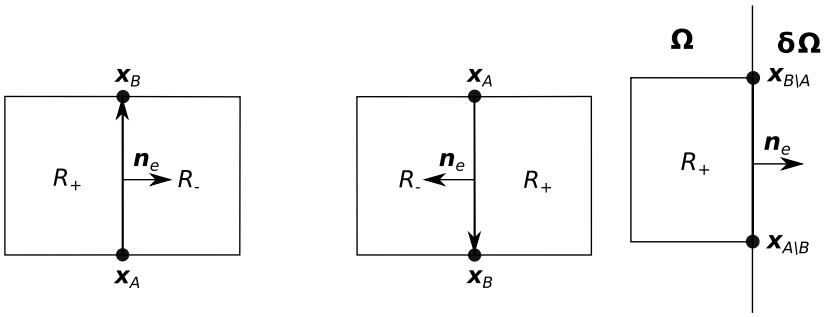

(a) Support on interior edges

(b) Support on boundary edges

Figure 3.5: Support of the roof basis function

Similarly as in [1, def. 4.2] for the triangular case, we define the support of a shape function of the lowest order Raviart-Thomas space.

Definition 3.16 (Support of edge basis functions) *Let $\mathcal{R} = (\Theta, \mathcal{E})$ be a rectangulation of $\Omega \subset \mathbb{R}^2$ and let $e \in \mathcal{E}$.*

If e is an interior edge oriented from $\mathbf{x}_A$ to $\mathbf{x}_B$, i. e. , $e = \overrightarrow{(\mathbf{x}_A, \mathbf{x}_B)} \notin \partial\Omega$, let

$$R_\pm := conv\{e \cup e_\pm\} \quad \text{for } e_\pm \text{ the edge oppoisite to } e \tag{3.22a}$$
such that
R_+ is the left and R_- the right neighbouring elemenet of e and
$\mathbf{n}_e$ the outwards pointing unit normal vector on $e \cap \partial R_+$.

If e is a boundary edge , i. e. , $e \in \partial\Omega$, let

$$R_+ := \{R \in \mathcal{R} |\ e \subset \partial R\}, \tag{3.22b}$$
$\mathbf{n}_e$ *is the outwardpointing unit normal vector on R_+ and R_- is not defined in this case.*

For interior edges the direction of $\mathbf{n}_e$ changes with the orientation of e and is uniquely given by the choice of $R_\pm$, as illustrated in figure 3.5.
To the best of her knowledge the author could not find an explicit form of a basis of conforming bilinear lowest order Raviart-Thomas elements in the literature. Therefore similarly as in [1, def. 4.3] a basis was constructed with a different normalization condition, due to the later proceeding.

Definition 3.17 (Roof functions) *Let $\mathcal{R} = (\Theta, \mathcal{E})$, $e = \overrightarrow{(\mathbf{x}_A, \mathbf{x}_B)} \in \mathcal{E}$, $R_\pm$ be given as above define*

$$\mathbf{b}_e(\mathbf{x}) := \begin{cases} \frac{1}{|e|}\left(1 - \frac{2|T_{x,x_A,x_B}|}{|R_\pm|}\right)\mathbf{n}_e & \text{for} \quad \mathbf{x} \in R_\pm, \\ 0 & \text{for} \quad \mathbf{x} \in \Omega \setminus R_\pm, \end{cases} \tag{3.23}$$

where $T_{x,x_A,x_B} = conv\{\mathbf{x}, \mathbf{x}_A, \mathbf{x}_B\}$, is the triangle spanned by $\mathbf{x}$, $\mathbf{x}_A$ and $\mathbf{x}_B$.

Proposition 3.18 *Let $\mathcal{R} = (\Theta, \mathcal{E})$, $e = \overrightarrow{(\mathbf{x}_A, \mathbf{x}_B)} \in \mathcal{E}$, $R_\pm$ be given as in definition 3.16, then the area of the triangle $T_{x,x_A,x_B} = conv\{\mathbf{x}, \mathbf{x}_A, \mathbf{x}_B\}$ for $\mathbf{x} \in R_\pm$ can be written as*

$$|T_{x,x_A,x_B}| = \frac{1}{2}|R_\pm|F^{-1}(\mathbf{x})^2 \quad \text{for} \quad \mathbf{x} \in R_\pm, \tag{3.24}$$

where $F : \hat{R} \to R_\pm$ is the affine transformations which maps the reference rectangle to $R_\pm$, such that $F((0,0)^\intercal) = \mathbf{x}_A$ and $F((1,0)^\intercal) = \mathbf{x}_B$.

Proof Let $R_\pm$, e and $\mathbf{x}$ be given as above and let $e' \in R_\pm$ be an edge orthogonal to e. Then

$$|T_{x,x_A,x_B}| = \frac{1}{2}|e|\text{dist}(e, \mathbf{x}). \tag{3.25}$$

We have $\text{dist}(e, \mathbf{x}) = |e'|F^{-1}(\mathbf{x})^2$, because $F((0,0)^\intercal) = \mathbf{x}_A$ and $F((1,0)^\intercal) = \mathbf{x}_B$ as illustrated in figure 3.6 and therefore it follows

$$|T_{x,x_A,x_B}| = \frac{1}{2}|e||e'|F^{-1}(\mathbf{x})^2 = \frac{1}{2}|R_\pm|F^{-1}(\mathbf{x})^2. \qquad \square$$

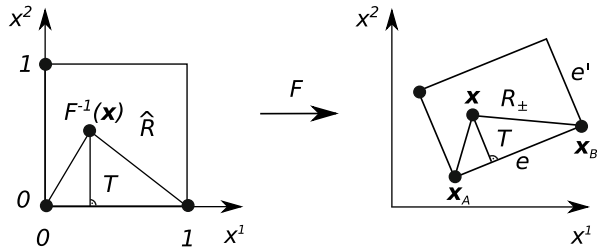

Figure 3.6: Rectangle under affine transformation

Theorem 3.19 *Let $\mathcal{R} = (\Theta, \mathcal{E})$ be a rectangulation of Ω, let $e \in \mathcal{E}$ and $\mathbf{b}_e$ be given as in def. 3.17. Then*

i) for all $f \in \mathcal{E}$ $\quad \mathbf{b}_e \cdot \mathbf{n}_f(\mathbf{x})|_f = \frac{1}{|e|}\delta_{e,f}$,

ii) $\mathbf{b}_e \in H(div, \Omega)$,

iii) $\{\mathbf{b}_e\}_{e\in\mathcal{E}}$ *is a basis of* $\mathcal{RT}_0(\Omega,\mathcal{R})$,

iv) $div(\mathbf{b}_e)(\mathbf{x}) := \begin{cases} \pm\dfrac{1}{|R_\pm|} & for \quad \mathbf{x}\in R_\pm, \\ 0 & for \quad \mathbf{x}\in\Omega\setminus R_\pm \quad and \end{cases}$

v) $\int_e \mathbf{b}_e(\mathbf{x})\cdot\mathbf{n} \quad d\sigma(\mathbf{x}) = 1.$

Proof Let $e\in\mathcal{E}$ be an edge in the rectangulation of Ω.

i) This proof follows the idea of the proof [1, lem. 4.1].
Assume $\mathbf{x}\in e\subset R_\pm$, then

$$\mathbf{b}_e\cdot\mathbf{n}_e(\mathbf{x}) = \frac{1}{|e|}\big(1-\frac{2|T_{x,x_A,x_B}|}{|R_\pm|}\big)\mathbf{n}_e\cdot\mathbf{n}_e.$$

Note that $|T_{x,x_A,x_B}| = 0$ for $\mathbf{x}\in e = \overrightarrow{(\mathbf{x}_A,\mathbf{x}_B)}$ and recall $\mathbf{n}_e$ is normalized. It follows

$$\mathbf{b}_e\cdot\mathbf{n}_e(\mathbf{x}) = \frac{1}{|e|}(1-0) = \frac{1}{|e|}.$$

On the one hand, let $f\in\mathcal{E}$ be an edge different form e orthogonal to e, let $\mathbf{x}\in f\neq e$ and $f\subset R_+\cup R_-$. Then $\mathbf{n}_e\cdot\mathbf{n}_f = 0$, thus it is concluded

$$\mathbf{b}_e\cdot\mathbf{n}_f(\mathbf{x}) = \frac{1}{|e|}\big(1-\frac{2|T_{x,x_A,x_B}|}{|R_\pm|}\big)\mathbf{n}_f\cdot\mathbf{n}_e = 0.$$

On the other hand, for $f\in\mathcal{E}$ an edge different form e, parallel to e, $\mathbf{x}\in f\neq e$ and $f\subset R_+\cup R_-$, it can be written $|T_{x,x_A,x_B}| = \frac{1}{2}|R_\pm|$, since f is an edge parallel to e, whence $F^{-1}(\mathbf{x})^2 = 1$ and

$$\mathbf{b}_e\cdot\mathbf{n}_f(\mathbf{x}) = \frac{1}{|e|}\big(1-\frac{2|T_{x,x_A,x_B}|}{|R_\pm|}\big)\mathbf{n}_e\cdot\mathbf{n}_f = \frac{1}{|e|}\big(1-\frac{|R_\pm|}{|R_\pm|}\big)\mathbf{n}_e\cdot\mathbf{n}_f = 0.$$

It remains to show the claim for f not an edge in the support of $\mathbf{b}_e$. Recall that $\mathbf{b}_e(\mathbf{x})$ vanishes for $\mathbf{x}\notin R_+\cup R_-$, which finishes the proof.

ii) and iii) can be proven as [1, lem. 4.1 b) and c)] with slight modifications, therefore they are not stated in this work.

iv) Assume $e\in\mathcal{E}$ and $\mathbf{x}\in R_\pm$. Inserting eq. (3.25) into (3.23), it can be written

$$\mathbf{b}_e(\mathbf{x}) = \frac{1}{|e|}\big(1-F^{-1}(\mathbf{x})^2\big)\cdot\mathbf{n}_e.$$

Therefore $\mathbf{b}_e$ is continuous differentiable on $R_\pm^\circ$ an the divergence theorem may be applied:

$$\int_{R_\pm} \operatorname{div}(\mathbf{b}_e)(\mathbf{x})\, d\mathbf{x} = \int_{\partial R_\pm} \frac{1}{|e|}\big(1 - F^{-1}(\mathbf{x})^2\big)\mathbf{n}_e \cdot \mathbf{n}\, d\sigma(\mathbf{x}).$$

Furthermore, as show in ii) $\mathbf{b}_e$ is linear and its divergence is constant on its support, therefore

$$|R_\pm| \operatorname{div}(\mathbf{b}_e) = \int_{\partial R_\pm} \frac{1}{|e|}\big(1 - F^{-1}(\mathbf{x})^2\big)\mathbf{n}_e \cdot \mathbf{n}\, d\sigma(\mathbf{x}),$$

where $\mathbf{n}$ denotes the outwards pointing unit normal vector of $\partial R_\pm$. Since $\mathbf{n} \cdot \mathbf{n}_e = \pm 1$ on $\partial R_\pm$ by the definition of $\mathbf{n}_e$ (eq. (3.22)) and applying the substitution of variables formula $\mathbf{y} = F^{-1}(\mathbf{x})$ and $\frac{d\sigma(\mathbf{x})}{d\sigma(\mathbf{y})} = |e|$ as illustrated in figure 3.6, it follows that

$$\begin{aligned}
\operatorname{div}(\mathbf{b}_e) &= \pm\frac{1}{|R_\pm|} \int_{[0,1]\times\{0\}\cup[0,1]\times\{1\}} 1 - y^2\, d\sigma(\mathbf{y}) \\
&= \pm\frac{1}{|R_\pm|}\big((1-0) + (1-1)\big) \\
&= \pm\frac{1}{|R_\pm|}.
\end{aligned}$$

For $\mathbf{x} \in \Omega \setminus R_\pm$, we have $\mathbf{b}_e(\mathbf{x}) = 0$ and there is nothing to show.

v) For any $e \in \mathcal{E}$ by the definition of $\mathbf{b}_e$, its continuity at interfaces and prop. 3.18 we have

$$\int_e \mathbf{b}_e(\mathbf{x}) \cdot \mathbf{n}\, d\sigma(\mathbf{x}) = \int_e \mathbf{b}_e(\mathbf{x}) \cdot \mathbf{n}_e\, d\sigma(\mathbf{x}) = \int_e \frac{1}{|e|}\big(1 - F^{-1}(\mathbf{x})^2\big)\, d\sigma(\mathbf{x}).$$

Once again, applying the integration by substitution formula $\mathbf{y} = F^{-1}(\mathbf{x})$ and $\frac{d\sigma(\mathbf{x})}{d\sigma(\mathbf{y})} = |e|$, it is obtained that

$$\begin{aligned}
\int_e \mathbf{b}_e(\mathbf{x}) \cdot \mathbf{n}\, d\sigma(\mathbf{x}) &= \int_{[0,1]\times\{0\}} 1 - y^2\, d\sigma(\mathbf{y}) \\
&= 1 - 0 \\
&= 1.
\end{aligned}$$

□

As shown in the first part of the proof of i), edge basis elements are constant on their associated edges:

Proposition 3.20 *For $\mathbf{b}_e$, $e \in \mathcal{E}$ an element of the roof basis*

$$\mathbf{b}_e(\mathbf{x})|_e = \frac{1}{|e|}\mathbf{n}_e. \tag{3.27}$$

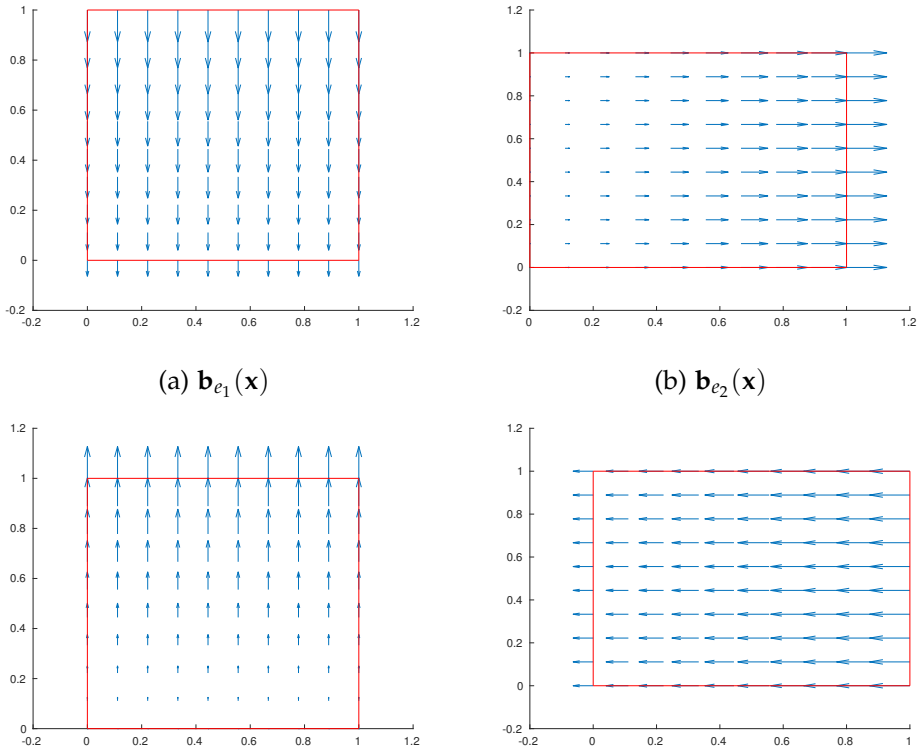

(a) $\mathbf{b}_{e_1}(\mathbf{x})$ (b) $\mathbf{b}_{e_2}(\mathbf{x})$

(c) $\mathbf{b}_{e_3}(\mathbf{x})$ (d) $\mathbf{b}_{e_4}(\mathbf{x})$

Figure 3.7: Roof functions on the reference element

In the proof of iv) it was used that the basis functions by definition 3.16 satisfy the following:

Proposition 3.21 *Let Ω be a domain with boundary $\partial\Omega$ oriented such that Ω is left to $\partial\Omega$ and let $\mathbf{n}$ be the outwards pointing unit normal vector on $\partial\Omega$. Then for any rectangulation $\mathcal{R} = (\Theta, \mathcal{E})$ of Ω*

$$\mathbf{n}_e \cdot \mathbf{n} = 1 \quad \textit{and} \tag{3.28a}$$

$$sgn(div(\mathbf{b}_e)) = 1 \quad \textit{for all} \quad e \in \mathcal{E} \cap \partial\Omega. \tag{3.28b}$$

The four roof function on the reference element with $\Omega = \hat{R}$ are plotted in figure 3.7. The edges are labeled by $e_1 = \overrightarrow{((0,0)^\intercal, (1,0)^\intercal)}$, $e_2 = \overrightarrow{((1,0)^\intercal, (1,1)^\intercal)}$, $e_3 = \overrightarrow{((1,1)^\intercal, (0,1)^\intercal)}$ and $e_4 = \overrightarrow{((0,1)^\intercal, (0,0)^\intercal)}$.

Chapter 4

Virtual Gap Technique

In this work we use the technique known as the virtual gap technique, that is, assuming the primal domain is a separation line. Applied to the previously used model problem the unit square is partitioned so that the primal domain separates multiple dual domains. To enable a coupling among the dual variables on the dual sub domains, the primal domain's width is considered as vanishing. The technique is illustrated in figure 4.1.
In this chapter in section 4.1 the separation of the domain is defined, the linear system associated with the Galerkin discretization of this problem derived in detail in section 4.2 and in section 4.3 the limiting process is discussed.

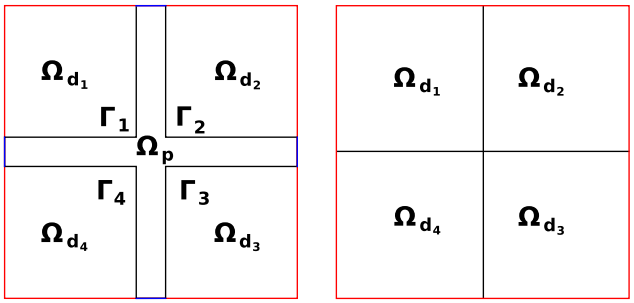

(a) Partition (b) Virtual gap

Figure 4.1: Virtual gap technique applied to a partition.

4.1 Partition I

For $1 \gg \delta > 0$, let the following partition of the domain $\Omega = (0,1)^2$ be given:
$\Omega_5 = (0.5 - \frac{\delta}{2}, 0.5 + \frac{\delta}{2}) \times (0,1) \cup (0,1) \times (0.5 - \frac{\delta}{2}, 0.5 + \frac{\delta}{2})$ and Ω_i for $1 \leq i \leq$

4 are the disjoint subsets of $(\Omega \setminus \Omega_5)^\circ$, numbered clockwise as in figure 4.2. Let $\Gamma_i = \partial\Omega_i \cap \partial\Omega_5$ and $\mathbf{n}_i$ be the outwards pointing unit normal vectors on $\partial\Omega_i$ for $1 \leq i \leq 4$ and define $\Gamma := \Gamma_1 \cap \Gamma_2 \cap \Gamma_3 \cap \Gamma_4$, the coupling boundary. $\mathbf{n}$ denotes the outwards pointing unit normal vector on $\partial\Omega_5$.

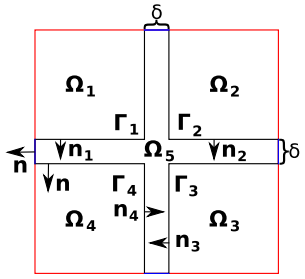

Figure 4.2: Partition I

4.1.1 Galerkin Discretization on Partition I

We assume that Ω_5 is the primal domain and Ω_i for $1 \leq i \leq 4$ are the dual domains.

Proposition 4.1 *Let u_5 be the primal variable and u_i for $1 \leq i \leq 4$ be the dual variables. Then the discretized weak formulation of the BVP imposed by Poission's equation (eq. 2.22) writes as:*

Find $(\mathbf{j}_{h_5}, u_{h_5}, u_{h_1}, u_{h_2}, u_{h_3}, u_{h_4}) \in \mathcal{RT}_0(\Omega_5, \mathcal{R}_{h_5}) \times W_0(\Omega_5, \mathcal{R}_{h_5})$
$\times\, S^1_{0;\partial\Omega_1\setminus\Gamma_1}(\Omega_1, \mathcal{T}_{h_1}) \times S^1_{0;\partial\Omega_2\setminus\Gamma_2}(\Omega_2, \mathcal{T}_{h_2}) \times S^1_{0;\partial\Omega_3\setminus\Gamma_3}(\Omega_3, \mathcal{T}_{h_3}) \times S^1_{0;\partial\Omega_4\setminus\Gamma_4}(\Omega_4, \mathcal{T}_{h_4})$
such that

$$\int_{\Omega_5} \mathbf{j}_{h_5} \cdot \mathbf{q}_{h_5} + \int_{\Omega_5} div(\mathbf{q}_{h_5}) u_{h_5}\, d\mathbf{x} - \sum_{i=1}^{4} \int_{\Gamma_i} \mathbf{q}_{h_5} u_{h_i} \cdot \mathbf{n}\, d\sigma(\mathbf{x}) = 0 \tag{4.1a}$$

$$\text{for all} \quad \mathbf{q}_{h_5} \in \mathcal{RT}(\Omega_5, \mathcal{R}_{h_5}),$$

$$\int_{\Omega_5} div(\mathbf{j}_{h_5}) v_{h_5}\, d\mathbf{x} = -\int_{\Omega_5} f v_{h_5}\, d\mathbf{x} \tag{4.1b}$$

$$\text{for all} \quad v_{h_5} \in W_0(\Omega_5, \mathcal{R}_{h_5}) \quad \text{and}$$

$$-\int_{\Gamma_i} \mathbf{j}_{h_5} v_{h_i} \cdot \mathbf{n}\, d\sigma - \int_{\Omega_i} \nabla u_{h_i} \cdot \nabla v_{h_i}\, d\mathbf{x} = -\int_{\Omega_i} f v_{h_i}\, d\mathbf{x} \tag{4.1c}$$

$$\text{for all} \quad v_{h_i} \in S^1_{0;\partial\Omega_i\setminus\Gamma_i}(\Omega_i, \mathcal{T}_{h_i}), \quad \text{for} \quad 1 \leq i \leq 4.$$

Proof Since the Galerkin discretized version of the saddle point problem directly follows from the restriction of the search space, it suffice to show

that the solution of the BVP given by the primal u_5 and the dual variables u_i for $1 \leq i \leq 4$ satisfy the above saddle point problem in the weak sense. Let $u_i \in H^1_{0;\partial\Omega_i\setminus\Gamma_i}(\Omega_i)$, respectively $u_5 \in H^0(\Omega_5)$, be the solution of the PDE system imposed by eq. (2.3) on Ω_i for $1 \leq i \leq 4$, respectively eq. (2.2) on Ω_5. By Green's formula (lem. 2.12) for all $\mathbf{q}_5 \in H(\mathrm{div};\Omega_5)$ we have

$$\int_{\Omega_5} \mathrm{div}(\mathbf{q}_5)u_5 + \mathbf{q}_5 \cdot \nabla u_5 \quad d\mathbf{x} = \int_{\partial\Omega_5} \mathbf{q}_5 u_5 \cdot \mathbf{n} \quad d\sigma(\mathbf{x}).$$

Let $\mathbf{j_5} = \nabla u_5$ denote the flux in Ω_5 and recall, due to the BCs, $u_5|_{\Gamma_i} = u_i$ for $1 \leq i \leq 4$, whereas $u_5|_{\partial\Omega_5\setminus\Gamma} = 0$, it follows that

$$\int_{\Omega_5} \mathbf{j}_5 \cdot \mathbf{q}_5 \, d\mathbf{x} + \int_{\Omega_5} \mathrm{div}(\mathbf{q}_5)u_5 \, d\mathbf{x} - \sum_{i=1}^{4} \int_{\Gamma_i} \mathbf{q}_5 u_i \cdot \mathbf{n} \, d\sigma(\mathbf{x}) = 0.$$

Let $v_5 \in H^0(\Omega_5)$. By multiplying Poission's equation (2.22a) with v_5, integrating and inserting the flux $\mathbf{j}_5$ it is obtained

$$\int_{\Omega_5} div(\mathbf{j}_5)v_5 \, d\mathbf{x} = -\int_{\Omega_5} f v_5 \, d\mathbf{x}.$$

Moreover for $1 \leq i \leq 4$, let $v_i \in H^1_{0;\partial\Omega_i\setminus\Gamma_i}(\Omega_i)$. Multiplying Poission's equation with v_i and integrating over Ω_i it can be written

$$-\int_{\Omega_i} \Delta u_i v_i \, d\mathbf{x} = \int_{\Omega_i} f v_i \, d\mathbf{x}.$$

By partial integration and the boundary condition given by eq. (2.3b) it is derived that

$$-\int_{\Gamma_i} \mathbf{j}_5 v_i \cdot \mathbf{n} \, d\sigma - \int_{\Omega_i} \nabla u_i \cdot \nabla v_i \, d\mathbf{x} = -\int_{\Omega_i} f v_i \, d\mathbf{x}. \qquad \square$$

The Galerkin discretized problem is given by a symmetric linear system for the degrees of freedom on the sub domains.

Lemma 4.2 *Let $\mathcal{T}_{h_i} = (\Theta_{h_i}, \mathcal{E}_{h_i})$, $n_i = |\Theta^\circ_{h_i}|$ for $1 \leq i \leq 4$, $N = \sum_{i=1}^4 n_i$, $\mathcal{R}_{h_5} = (\Theta_{h_5}, \mathcal{E}_{h_5})$, $M = |\mathcal{E}_{h_5}|$ and define $O = |\mathcal{R}_{h_5}|$. Let $\{b^{\circ,i}_{x_k}\}_{x_k \in \Theta^\circ_i}$ be the hat functions basis of $S^1_{0;\partial\Omega_i\setminus\Gamma_i}(\Omega_{h_i}, \mathcal{T}_{h_i})$ for $1 \leq i \leq 4$, $\{\mathbf{b}_{e_p}\}_{e_p \in \mathcal{E}_{h_5}}$ denote the roof functions basis of $\mathcal{RT}_0(\Omega_5, \mathcal{R}_{h_5})$ and let $\{b_{R_j}\}_{R_j \in \mathcal{R}_{h_5}}$ be the standard basis of $W_0(\Omega_5, \mathcal{R}_{h_5})$ as defined in lemma 3.14. Then the discretized problem is equivalent*

to:

$$\textit{Find} \quad \mathbf{u} \in \mathbb{R}^{N+O+M} \quad \textit{such that} \quad A\mathbf{u} = \mathbf{l} \quad \textit{for} \tag{4.2a}$$

$$A = \begin{pmatrix} A^1 & 0 & 0 & 0 & 0 & B^{15} \\ 0 & A^2 & 0 & 0 & 0 & B^{25} \\ 0 & 0 & A^3 & 0 & 0 & B^{35} \\ 0 & 0 & 0 & A^4 & 0 & B^{45} \\ 0 & 0 & 0 & 0 & 0 & B^5 \\ (B^{15})^\intercal & (B^{25})^\intercal & (B^{35})^\intercal & (B^{45})^\intercal & (B^5)^\intercal & A^5 \end{pmatrix}, \tag{4.2b}$$

$$\mathbf{u} = \begin{pmatrix} \underline{\alpha}^1 \\ \underline{\alpha}^2 \\ \underline{\alpha}^3 \\ \underline{\alpha}^4 \\ \underline{\beta} \\ \underline{\gamma} \end{pmatrix}, \quad \underline{\alpha}^i \in \mathbb{R}^{n_i}, \quad \underline{\beta} \in \mathbb{R}^O, \quad \underline{\gamma} \in \mathbb{R}^M, \quad \mathbf{l} = \begin{pmatrix} \mathbf{l}^1 \\ \mathbf{l}^2 \\ \mathbf{l}^3 \\ \mathbf{l}^4 \\ \mathbf{l}^5 \\ \mathbf{0} \end{pmatrix}, \tag{4.2c}$$

$$A^i_{k_i,l_i} := -\int_{\Omega_i} \nabla b^{\circ,i}_{x_{k_i}}(\mathbf{x}) \cdot \nabla b^{\circ,i}_{x_{l_i}}(\mathbf{x})\, d\mathbf{x}, \tag{4.2d}$$

$$l^i_{k_i} := \int_{\Omega_i} f(\mathbf{x}) b^{\circ,i}_{x_{k_i}}(\mathbf{x}) \quad d\mathbf{x}, \tag{4.2e}$$

$$A^5_{p,q} := \int_{\Omega_5} \mathbf{b}_{e_q}(\mathbf{x}) \cdot \mathbf{b}_{e_p}(\mathbf{x})\, d\mathbf{x}, \tag{4.2f}$$

$$B^{i,5}_{k_i,p} := -\int_{\Gamma_i} \mathbf{b}_{e_p}(\mathbf{x}) b^{\circ,i}_{x_{k_i}}(\mathbf{x}) \cdot \mathbf{n}\, d\sigma(\mathbf{x}), \tag{4.2g}$$

$$B^5_{j,p} := \int_{\Omega_5} div(\mathbf{b}_{e_p})(\mathbf{x}) b_{R_j}(\mathbf{x})\, d\mathbf{x}, \tag{4.2h}$$

$$l^5_j := -\int_{\Omega_5} f(\mathbf{x}) b_{R_j}(\mathbf{x})\, d\mathbf{x}, \tag{4.2i}$$

$$\textit{where} \quad 1 \le i \le 4, \quad 1 \le k_i, l_i \le n_i, \quad 1 \le p, q \le M \quad \textit{and} \quad 1 \le j \le O.$$

Moreover

$$u_{h_i}(\mathbf{x}) = \sum_{i=1}^{n_i} \alpha^i_{k_i} b^{\circ,i}_{x_{k_i}}(\mathbf{x}) \quad \textit{for} \quad 1 \le i \le 4, \tag{4.2j}$$

$$\mathbf{j}_{h_5}(\mathbf{x}) = \sum_{p=1}^{M} \gamma_p \mathbf{b}_{e_p}(\mathbf{x}) \quad \textit{and} \tag{4.2k}$$

$$u_{h_5}(\mathbf{x}) = \sum_{j=1}^{O} \beta_j b_{R_j}(\mathbf{x}). \tag{4.2l}$$

Proof Due to the lengthy formula the idea of this proof is stated.
This lemma can be proven by first representing the solution of the discretization problem by the basis functions defined in chapter 3, as written

in eq. (4.2j)- (4.2k) and second using that eq. (4.2) is satisfied for every $\mathbf{q}_{h_5} \in \mathcal{RT}_0(\Omega_5, \mathcal{R}_{h_5})$, $v_{h_i} \in S^1_{0;\partial\Omega_i\setminus\Gamma_i}(\Omega_i, \mathcal{T}_{h_i})$, for $1 \leq i \leq 4$, respectively $v_{h_5} \in W_0(\Omega, \mathcal{R}_{h_5})$ if and only if it is satisfied for every element of a basis $\{\mathbf{b}_{e_p}\}_{e_p\in\mathcal{E}_{h_5}}$, $\{b^{\circ,i}_{x_{k_i}}\}_{x_{k_i}\in\Theta^\circ_{h_i}}$ respectively $\{u_{R_j}\}_{R_j\in\mathcal{R}_{h_5}}$. This follows, because as in chp. 2 the weak formulation is equivalent to a variational formulation using bilinear forms like in eq. (2.21).
Finally, it is made use of the formula of matrix-vector multiplication, i. e. , $B\mathbf{v} = \mathbf{w}$ for $B \in \mathbb{R}^{d\times d}$ and $\mathbf{v}, \mathbf{w} \in \mathbb{R}^d$ is equivalent to

$$\sum_{k=1}^{d} B_{j,k}v^k = w^j \quad \text{for all} \quad 1 \leq j \leq d.$$

Defining matrices and vectors as in eq. (4.2d) - (4.2i) and comparing the indices it follows

$$A^i\underline{\alpha}^i + B^{i,5}\underline{\gamma} = \underline{l}^i \quad \text{for} \quad \underline{\alpha}^i \in \mathbb{R}^{n_i}, \underline{\beta} \in \mathbb{R}^O \quad \text{and} \quad \underline{\gamma} \in \mathbb{R}^M$$

is equivalent to equation (4.1c),

$$B^5\underline{\beta} = \underline{l}^5 \quad \text{for} \quad \underline{\beta} \in \mathbb{R}^O$$

is equivalent to eq. (4.1b) and

$$\sum_{i=1}^{4}(B^{i,5})^\intercal\underline{\alpha}^i + (B^5)^\intercal\underline{\beta}^5 + A^5\underline{\gamma} = \mathbf{0} \quad \text{for} \quad \underline{\alpha}^i \in \mathbb{R}^{n_i}, \underline{\beta} \in \mathbb{R}^O \quad \text{and} \quad \underline{\gamma} \in \mathbb{R}^M$$

is equivalent to eq. (4.1a). □

A, A^i, A^5, $B^{i,5}$, B^5 are called *stiffness matrices* of the underlying FEM.
In the following the subindex i is not written out if avoidable for simplification.

4.2 Virtual Gap

The sub domain Ω_5 is the vitual gap in partition I. Therefore $|e_p| = \delta \quad \text{for} \quad e_p \subseteq \mathcal{E}_{h_5} \setminus \Gamma$ and a limiting process $\delta \to 0$, is considered. The edges of vanishing length are illustrated in figure 4.3.

First the local stiffness matrices, which give the contribution of the shape functions on single elements in the partition, are calculated in section two of this chapter. The local linear FEM stiffness matrices of the dual domains are calculated in subsection 4.2.1, the linear FEM and Raviart-Thomas FEM coupling stiffness matrix elements on the coupling boundary are derived in subsection 4.2.2, the Raviart-Thomas constant FEM coupling stiffness matrices in 4.2.3 and the Raviart-Thomas stiffness matrices in 4.2.4.

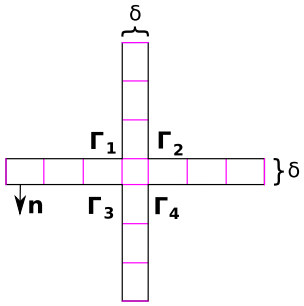

Figure 4.3: Illustration of the virtual gap: The edges of vanishing length are colored.

4.2.1 Linear Finite Elements Stiffness Matrix

The stiffness matricies A^i elements for $1 \leq i \leq 4$ of the linear FEM are given by

$$-\int_{\Omega_i} \nabla b^{\circ}_{x_k}(\mathbf{x}) \cdot \nabla b^{\circ}_{x_l}(\mathbf{x})\, d\mathbf{x} \quad \text{for} \quad 1 \leq k, l \leq n, \tag{4.3}$$

which is the negative element matrix for the Laplacian. Since a routine for generating this matrix on a triangular mesh is provides by LehrFEM, using the command `STIMA_Lapl_LFM` [4, chp. 4.1.4], it is not treated.

4.2.2 Linear Finite Elements - Raviart-Thomas Finite Elements Stiffness Matrix in the Gap

Note that only for $e, \mathbf{x_k} \subset \Gamma_i$ the matrix elements, which couple the linear FEMs with Raviart-Thomas FEMs, do not vanish, hence for $1 \leq i \leq 4$

$$B^{i,5}_{k,p} = \begin{cases} -\int_{e_p \cap \mathrm{supp}(b_{x_k})} \mathbf{b}_{e_p}(\mathbf{x}) b^{\circ,i}_{x_k}(\mathbf{x}) \cdot \mathbf{n}\, d\sigma(\mathbf{x}) & \text{if} \quad e_p, \mathbf{x}_k \subset \Gamma_i, \\ 0 & \text{if} \quad e_p, \mathbf{x}_k \subset \Omega \setminus \Gamma_i. \end{cases} \tag{4.4}$$

Because of proposition 3.21 and 3.20 the above integral reduces to

$$-\frac{1}{|e_p|} \int_{e_p \cap \mathrm{supp}(b^{\circ,i}_{x_k})} b^{\circ,i}_{x_k}(\mathbf{x})\, d\sigma(\mathbf{x}). \tag{4.5}$$

4.2.3 Raviat-Thomas Elements - Piecewise Constant Finite Elements Stiffness Matrix in the Gap

Let $R_{\pm}(e_p)$ denote the support of e_p, for e_p some edge in $\mathcal{E}_5$, using theorem 3.19, iv) and eq (3.20) it follows

$$B^5_{j,p} = \int_{\Omega_5} \operatorname{div}(\mathbf{b}_{e_p})(\mathbf{x}) b_{R_j}(\mathbf{x})\, d\mathbf{x} \tag{4.6}$$

$$= \begin{cases} \pm \int_{R_j} \frac{1}{|R_j|}\, d\mathbf{x} & \text{if} \quad e_p \subset R_j \quad \text{and} \quad R_j = R_{\pm}(e_p), \\ 0 & \text{if} \quad e_p \not\subseteq R_j. \end{cases} \tag{4.7}$$

$$= \begin{cases} \pm 1 & \text{if} \quad e_p \subset R_j \quad \text{and} \quad R_j = R_{\pm}(e_p), \\ 0 & \text{if} \quad e_p \not\subseteq R_j. \end{cases} \tag{4.8}$$

Furthermore, by proposition 3.21 it is obtained the following:

Proposition 4.3 *Let $R = conv\{\mathbf{x}_1, \mathbf{x}_2, \mathbf{x}_3, \mathbf{x}_4\} \in \mathcal{R}_{h_5}$, $\mathbf{x}_1, ..., \mathbf{x}_4 \in \Theta_{h_5}$ be a rectangle, such that*

$$e_p = conv\{\mathbf{x}_p, \mathbf{x}_{p+1}\} \quad for \quad 1 \le p \le 4. \tag{4.9a}$$

Let the local stiffness matrix of $\mathcal{RT}_0(\Omega_5, \mathcal{R}_{h_5})$ and $W_0(\Omega_5, \mathcal{R}_{h_5})$ in the gap be

$$B^{5,R}_p := \int_R div(\mathbf{b}_{e_p})(\mathbf{x}) b_R(\mathbf{x})\, d\mathbf{x} \quad for \quad 1 \le p \le 4, \tag{4.9b}$$

then

$$B^{5,R}_p = \begin{cases} 1 & for \quad R = R_{\pm}(e_p) \quad and \quad e_p \subset \Gamma, \\ \pm 1 & for \quad R = R_{\pm}(e_p). \end{cases} \tag{4.9c}$$

4.2.4 Raviart-Thomas Element Stiffness Matrix in the Gap

Proposition 4.4 *Let $R = conv\{\mathbf{x}_1, \mathbf{x}_2, \mathbf{x}_3, \mathbf{x}_4\} \in \mathcal{R}_{h_5}$, $\mathbf{x}_1, ..., \mathbf{x}_4 \in \Theta_{h_5}$ be a rectangle, such that*

$$e_p = conv\{\mathbf{x}_p, \mathbf{x}_{p+1}\} \quad for \quad 1 \le p \le 4. \tag{4.10a}$$

Let the local coupling matrix of $\mathcal{RT}_0(\Omega_5, \mathcal{R}_{h_5})$ in the gap be

$$A^{5,R}_{p,q} := \int_R \mathbf{b}_{e_q}(\mathbf{x}) \cdot \mathbf{b}_{e_p}(\mathbf{x})\, d\mathbf{x} \quad for \quad 1 \le p, q \le 4, \tag{4.10b}$$

then

$$A^{5,R}_{p,q} = \delta_{p,q} \frac{1}{3} \frac{|R|}{|e_p|^2} + \delta_{p,q+2} \mathbf{n}_p \cdot \mathbf{n}_q \frac{1}{6} \frac{|R|}{|e_p|^2}. \tag{4.10c}$$

Proof Note that due to the local numbering of the edges above, the parallel edges of R correspond to the entries on the second off diagonal of $A^{5,R}$.

Assume $R = R_{\pm}(e_p)$ for $e_p = \overrightarrow{(\mathbf{x}_A, \mathbf{x}_B)}$ and $F : \hat{R} \to R$ is the affine transformation as in proposition 3.18, then

$$\begin{aligned} A^{5,R}_{p,p} &= \int_R \mathbf{b}_{e_p}(\mathbf{x}) \cdot \mathbf{b}_{e_p}(\mathbf{x}) \quad d\mathbf{x} \\ &= \int_R \left(\frac{1}{|e_p|} (1 - \frac{2|T_{x,x_A,x_B}|}{|R|}) \mathbf{n}_e \right)^2 d\mathbf{x} = \frac{1}{|e_p|^2} \int_R \left(1 - \frac{|R| F^{-1}(\mathbf{x})^2}{|R|} \right)^2 d\mathbf{x} \\ &= \frac{1}{|e_p|^2} \int_R 1 - 2F^{-1}(\mathbf{x})^2 + (F^{-1}(\mathbf{x})^2)^2 \, d\mathbf{x}. \end{aligned}$$

Applying the integration by substitution formula $\mathbf{y} = F^{-1}(\mathbf{x})$, $\frac{d\mathbf{y}}{d\mathbf{x}} = |det(F'(\mathbf{x})| = |R|$ above constitutes to

$$\begin{aligned} &\frac{|R|}{|e_p|^2} \int_{[0,1]\times[0,1]} 1 - 2y^2 + (y^2)^2 \quad d\mathbf{y} = \frac{|R|}{|e_p|^2} \int_0^1 1 - 2z + z^2 dz \\ &= \frac{|R|}{|e_p|^2} (1 - 2\frac{1}{2} + \frac{1}{3}) = \frac{1}{3} \frac{|R|}{|e_p|^2}. \end{aligned}$$

Let $e_{p'} = \overrightarrow{(\mathbf{x}'_A, \mathbf{x}'_B)}$ denote an edge parallel to e_p in R. On the one hand from the parallelism of the edges it follows $\mathbf{n}_e \cdot \mathbf{n}_{e'} = \pm 1$, where the sign depends on the local orientation of both edges, and on the other hand $|T_{x,x'_A,x'_B}| = \frac{1}{2}|R|(1 - F^{-1}(\mathbf{x})^2)$ (see figure 4.4), whence

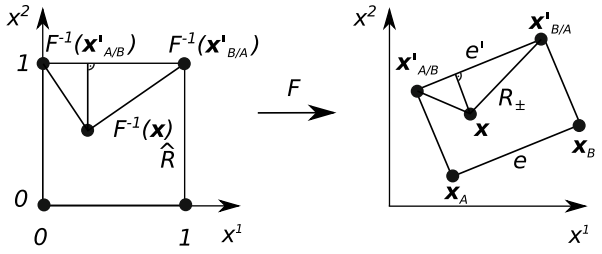

Figure 4.4: Rectangle under affine transformation

$$\begin{aligned} A^{5,R}_{p,p'} &= \int_R \mathbf{b}_{e_p}(\mathbf{x}) \cdot \mathbf{b}_{e_{p'}}(\mathbf{x}) \, d\mathbf{x} \\ &= \int_R \frac{1}{|e_p|} \left(1 - \frac{2|T_{x,x_A,x_B}|}{|R|} \right) \frac{1}{|e_{p'}|} \left(1 - \frac{2|T_{x,x'_A,x'_B}|}{|R|} \right) \mathbf{n}_{e_p} \cdot \mathbf{n}_{e_{p'}} \, d\mathbf{x} \\ &= \frac{\pm 1}{|e_p|^2} \int_R \left(1 - F^{-1}(\mathbf{x})^2\right) \left(1 - (1 - F^{-1}(\mathbf{x})^2)\right) \, d\mathbf{x} \\ &= \frac{\pm 1}{|e_p|^2} \int_R F^{-1}(\mathbf{x})^2 - \left(F^{-1}(\mathbf{x})^2\right)^2 \, d\mathbf{x}. \end{aligned}$$

Once again applying the substitution of variables formula as above, it is derived that

$$A^{5,R}_{p,p'} = \pm\frac{|R|}{|e_p|^2}\int_{[0,1]\times[0,1]} y^2 - (y^2)^2\, d\mathbf{y} = \pm\frac{|R|}{|e_p|^2}\int_0^1 z - z^2\, dz$$
$$= \pm\frac{|R|}{|e_p|}(\frac{1}{2}-\frac{1}{3}) = \frac{\pm 1}{6}\frac{|R|}{|e_p|^2}.$$

Note that for e_p orthogonal to e_q $\mathbf{b}_{e_p}\cdot\mathbf{b}_{e_q} = 0$, which finishes the proof. □

Proposition 4.5 *Let $e_p \neq e_q \in \mathcal{E}_5$ be two edges, then*

$$supp(\mathbf{b}_{e_p}) \cap supp(\mathbf{b}_{e_q}) = \begin{cases} R & \text{for some} \quad R \in \mathcal{R}_{h_5}, \\ \emptyset & \text{else.} \end{cases} \tag{4.11}$$

Proof Due to the length of this work only the idea is stated: This proposition can be show by contradiction, since every interior edge, has exactly two neighboring elements and therefore it separates them uniquely. □

Recall, that $\Omega_5 = \bigcup_{R_j\in\mathcal{R}} R_j$. It follows

$$A^5_{p,q} = \int_{\Omega_5} \mathbf{b}_{e_q}(\mathbf{x})\cdot\mathbf{b}_{e_p}(\mathbf{x})\, d\mathbf{x}$$
$$= \sum_{R_j\in\mathcal{R}} \int_{R_j} \mathbf{b}_{e_q}(\mathbf{x})\cdot\mathbf{b}_{e_p}(\mathbf{x})\, d\mathbf{x}. \tag{4.12}$$

Hence the local matrix contributes to the global matrix as in the following.

Proposition 4.6 *Let $e_p, e_q \in \mathcal{E}_{h_5}$ be two edges, the stiffness matrix associated to them writes as*

$$A^5_{p,q} = \begin{cases} A^{5,R}_{p,p} & if \quad p \neq q \quad for \quad R = supp(\mathbf{b}_{e_p}) \cap supp(\mathbf{b}_{e_q}), \\ A^{5,R_+(e_p)}_{p,p} + A^{5,R_-(e_p)}_{p,p} & if \quad p = q. \end{cases} \tag{4.13}$$

So far we derived the stiffness matrix entries of the coupling of the basis function associated to edges with respect to other edges, with respect to nodes in the dual mesh and with respect to midpoint of rectangles. Next we explore the coupling, if some edges have vanishing length.

4.3 Stiffness Matrix Scaling

In this section first, whereby an example, a stencil of the local stiffness matrices is shown, which occurs by introducing the virtual gap. This example is generalized in the next section and the general form of local stiffness matrix elements is derived. Last at the example of an equipartition virtual gap and dual mesh the stiffness matrix is explicitly calculated, applying the virtual gap technique to the Galerkin discretized problem imposed by partition I.

4.3.1 Diagonal Scaling the Raviart-Thomas Stiffness Matrix

Note that the entries of the coupling matrix of Raviart-Thomas elements in the gap depend on the length of the edges due to eq. (4.10b). In the following example the blow-up of the matrix entries due to a vanishing virtual gap width and an regularization by diagonal scaling the linear system given by the Galerkin discretized saddle point problem is demonstrated.

Let $R = \mathrm{conv}\{\mathbf{x}_1, \mathbf{x}_2, \mathbf{x}_3, \mathbf{x}_4\} \in \mathcal{R}_{h_5}$ be a rectangle in the gap, such that the pth local edge is the edge connecting $\mathbf{x}_p$ and $\mathbf{x}_{p+1}$. Furthermore let R lie in the gap, such that the local edges e_1 and e_3 lie on the coupling boundary and their width is given by $h = |e_1| = |e_3|$. As illustrated in figure 4.5 it is

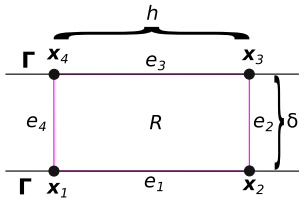

Figure 4.5: Rectangle with small hight

obtained that

$$\frac{|R|}{|e_p|^2} = \begin{cases} \dfrac{\delta h}{h^2} = \dfrac{\delta}{h} & \text{for} \quad p = 1, 3, \\ \dfrac{\delta h}{\delta^2} = \dfrac{h}{\delta} & \text{for} \quad p = 2, 4. \end{cases} \tag{4.14}$$

Therefore the coupling matrix of the edge basis function is given by

$$A^{5,R} = \begin{pmatrix} \frac{1}{3}\frac{\delta}{h} & 0 & \pm\frac{1}{6}\frac{\delta}{h} & 0 \\ 0 & \frac{1}{3}\frac{h}{\delta} & 0 & \pm\frac{1}{6}\frac{h}{\delta} \\ \pm\frac{1}{6}\frac{\delta}{h} & 0 & \frac{1}{3}\frac{\delta}{h} & 0 \\ 0 & \pm\frac{1}{6}\frac{h}{\delta} & 0 & \frac{1}{3}\frac{h}{\delta} \end{pmatrix}, \tag{4.15}$$

where the sign depends on the global orientation of the edges of R. In order to prevent a blow up of entries of order $O(\frac{1}{\delta})$ the 2nd and 4th row and column, corresponding to the edges of length δ are scaled by the factor $\sqrt{\delta}$ and the limit $\delta \to 0$ is taken. The scaled matrix $\tilde{A}^{5,R}$ then writes as

$$\tilde{A}^{5,R} = \begin{pmatrix} 0 & 0 & 0 & 0 \\ 0 & \frac{1}{3}h & 0 & \pm\frac{1}{6}h \\ 0 & 0 & 0 & 0 \\ 0 & \pm\frac{1}{6}h & 0 & \frac{1}{3}h \end{pmatrix}. \tag{4.16}$$

Note that the stencil of the local stiffness matrix is not unique, since the edge length is a local property given by the geometry of partition I (see

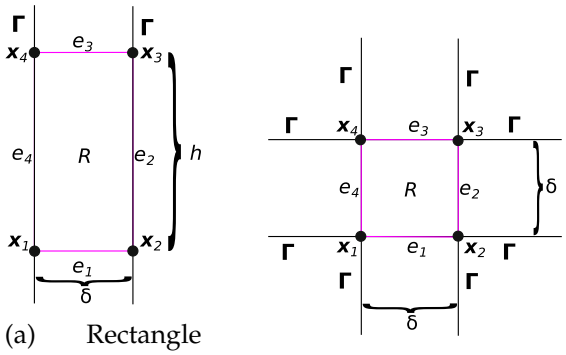

(a) Rectangle with small width

(b) Small square

Figure 4.6: Rectangles in partition I

figure 4.3). The other local alignments of rectangles are illustrated in figure 4.6a and 4.6b.

The corresponding two other occurring stencils are

$$\tilde{A}^{5,R} = \begin{pmatrix} \frac{1}{3}h & 0 & \pm\frac{1}{6}h & 0 \\ 0 & 0 & 0 & 0 \\ \pm\frac{1}{6}h & 0 & \frac{1}{3}h & 0 \\ 0 & 0 & 0 & 0 \end{pmatrix} \quad \text{and} \quad \tilde{A}^{5,R} = \begin{pmatrix} 0 & 0 & 0 & 0 \\ 0 & 0 & 0 & 0 \\ 0 & 0 & 0 & 0 \\ 0 & 0 & 0 & 0 \end{pmatrix}. \tag{4.17}$$

4.3.2 Scaled Matrix Structure

Since the solution of the linear system given by (4.2) of course must be invariant under the scaling of the rows and columns of matrix elements corresponding to edges of vanishing length, the scaling corresponds to transforming the left hand side of (4.2) by multiplication with a diagonal matrix.

Definition 4.7 *For $\delta > 0$ let the set of edges $\mathcal{E}_{h_5}$ be partitioned into the set of edges of small length $\mathcal{E}^{\delta}_{h_5}$ and the set of edges of non vanishing length $\mathcal{E}^{h_5}_{h_5}$, such that*

$$\begin{aligned} &\mathcal{E}^{\delta}_{h_5} = \{e \in \mathcal{E}_{h_5} |\ |e| = \delta\}, \quad \mathcal{E}^{h_5}_{h_5} = \{e \in \mathcal{E}_5 |\ |e| > \delta\}, \\ &\mathcal{E}_{h_5} = \mathcal{E}^{h_5}_{h_5} \cup \mathcal{E}^{\delta}_{h_5} \quad \textit{and} \quad \mathcal{E}^{h_5}_{h_5} \cap \mathcal{E}^{\delta}_{h_5} = \emptyset. \end{aligned} \tag{4.18}$$

Note that $\mathcal{E}^{h_5}_{h_5} = \mathcal{E}_{h_5} \cap \Gamma$ and $\mathcal{E}^{\delta}_{h_5} = \mathcal{E}_{h_5} \setminus (\mathcal{E}_{h_5} \cap \Gamma)$.

Lemma 4.8 *Let $A \in \mathbb{R}^{(N+O+M)\times(N+O+M)}$ be given as in (4.2), let $D^5 \in R^{M\times M}$*

be a diagonal matrix, such that

$$D^5_{p,p} = \begin{cases} \sqrt{\delta} & \text{if} \quad e_p \in \mathcal{E}^{\delta}_{h_5}, \\ 1 & \text{if} \quad e_p \in \mathcal{E}^{h_5} \end{cases} \quad \text{and let} \tag{4.19a}$$

$$D = \begin{pmatrix} 1 & 0 & \cdots & 0 \\ 0 & \ddots & \ddots & \vdots \\ \vdots & \ddots & 1 & 0 \\ 0 & \cdots & 0 & D^5 \end{pmatrix} \in \mathbb{R}^{(N+O+M)\times(N+O+M)}. \tag{4.19b}$$

$$\text{Define} \quad \tilde{A} := \lim_{\delta\to 0} DAD \quad \text{and} \quad \tilde{\mathbf{I}} = \lim_{\delta\to 0} D\mathbf{1}. \quad \text{Then} \tag{4.19c}$$

$$\tilde{A} = \begin{pmatrix} A^1 & 0 & 0 & 0 & 0 & B^{15} \\ 0 & A^2 & 0 & 0 & 0 & B^{25} \\ 0 & 0 & A^3 & 0 & 0 & B^{35} \\ 0 & 0 & 0 & A^4 & 0 & B^{45} \\ 0 & 0 & 0 & 0 & 0 & \tilde{B}^5 \\ (B^{15})^\intercal & (B^{25})^\intercal & (B^{35})^\intercal & (B^{45})^\intercal & (\tilde{B}^5)^\intercal & \tilde{A}^5 \end{pmatrix}, \tag{4.19d}$$

$$\text{where} \quad \tilde{A}^5 = \lim_{\delta\to 0} D^5 A^5 D^5 \quad \text{and} \quad \tilde{B}^5 = \lim_{\delta\to 0} B^5 D^5. \tag{4.19e}$$

$$\text{Furthermore} \quad \tilde{\mathbf{I}} = \mathbf{1} \quad \text{and for any} \tag{4.19f}$$

$$\tilde{\mathbf{w}} = \left(\underline{\alpha}^{1\intercal}, \ \underline{\alpha}^{2\intercal}, \ \underline{\alpha}^{3\intercal}, \ \underline{\alpha}^{4\intercal}, \ \underline{\beta}^{\intercal}, \ \underline{\tilde{\gamma}}^{\intercal}\right)^{\intercal}, \quad \text{which solves :}$$

$$\text{Find} \quad \tilde{\mathbf{u}} \in R^{(N+O+M)\times(N+O+M)}, \quad \text{such that} \quad \tilde{A}\tilde{\mathbf{u}} = \tilde{\mathbf{I}}. \tag{4.19g}$$

$$\text{We have} \quad \mathbf{w} = \left(\underline{\alpha}^{1\intercal}, \ \underline{\alpha}^{2\intercal}, \ \underline{\alpha}^{3\intercal}, \ \underline{\alpha}^{4\intercal}, \ \underline{\beta}^{\intercal}, \ (D^5\underline{\tilde{\gamma}})^{\intercal}\right)^{\intercal} \quad \text{solves} \quad (4.2). \tag{4.19h}$$

Proof First it is shown that taking the limit $\delta \to 0$ and the multiplication of A with D from left and right does only scale the blocks A^5 and B^5.
Let A be given as in (4.2b) and D be given as above. It can be written

$$\begin{aligned} \tilde{A} &= \lim_{\delta\to 0} DAD \\ &= \lim_{\delta\to 0} \begin{pmatrix} 1 & 0 & \cdots & \cdots & 0 \\ 0 & \ddots & \ddots & & \vdots \\ \vdots & \ddots & \ddots & \ddots & \vdots \\ \vdots & & \ddots & 1 & 0 \\ 0 & \cdots & \cdots & 0 & D^5 \end{pmatrix} \begin{pmatrix} A^1 & 0 & 0 & 0 & 0 & B^{15} \\ 0 & A^2 & 0 & 0 & 0 & B^{25} \\ 0 & 0 & A^3 & 0 & 0 & B^{35} \\ 0 & 0 & 0 & A^4 & 0 & B^{45} \\ 0 & 0 & 0 & 0 & 0 & B^5 \\ (B^{15})^\intercal & (B^{25})^\intercal & (B^{35})^\intercal & (B^{45})^\intercal & (B^5)^\intercal & A^5 \end{pmatrix} D \end{aligned}$$

$$= \lim_{\delta\to 0} \begin{pmatrix} A^1 & 0 & 0 & 0 & 0 & B^{15} \\ 0 & A^2 & 0 & 0 & 0 & B^{25} \\ 0 & 0 & A^3 & 0 & 0 & B^{35} \\ 0 & 0 & 0 & A^4 & 0 & B^{45} \\ 0 & 0 & 0 & 0 & 0 & B^5 \\ D^5(B^{15})^\intercal & D^5(B^{25})^\intercal & D^5(B^{35})^\intercal & D^5(B^{45})^\intercal & D^5(B^5)^\intercal & D^5A^5 \end{pmatrix}$$

$$\begin{pmatrix} 1 & 0 & \cdots & \cdots & 0 \\ 0 & \ddots & \ddots & & \vdots \\ \vdots & \ddots & \ddots & \ddots & \vdots \\ \vdots & & \ddots & 1 & 0 \\ 0 & \cdots & \cdots & 0 & D^5 \end{pmatrix}$$

$$= \lim_{\delta\to 0} \begin{pmatrix} A^1 & 0 & 0 & 0 & 0 & B^{15}D^5 \\ 0 & A^2 & 0 & 0 & 0 & B^{25}D^5 \\ 0 & 0 & A^3 & 0 & 0 & B^{35}D^5 \\ 0 & 0 & 0 & A^4 & 0 & B^{45}D^5 \\ 0 & 0 & 0 & 0 & 0 & B^5D^5 \\ D^5(B^{15})^\intercal & D^5(B^{25})^\intercal & D^5(B^{35})^\intercal & D^5(B^{45})^\intercal & D^5(B^5)^\intercal & D^5A^5D^5 \end{pmatrix}.$$

On the one hand by (4.19a) a multiplication from right with D^5 scales the pth column of a matrix if and only if $e_p \in \mathcal{E}^\delta_{h_5}$, therefore it follows using (4.4)

$$B^{i5}D^5_{k,p} = \begin{cases} \sqrt{\delta}B^{i,5}_{k,p} & if \quad e_p \in \mathcal{E}^\delta_{h_5}, \\ B^{i,5}_{k,p} & if \quad e_p \in \mathcal{E}^{h_5}_{h_5} \end{cases}$$
$$\text{for} \quad 1 \le i \le 4, \quad 1 \le k \le n \quad \text{and} \quad 1 \le p \le M.$$

Due to (4.4) $B^{i,5}_{k,p}$ vanishes if e_p does not lie on the coupling boundary Γ and therefore the scaling does not affect $B^{i,5}$, i. e. , $B^{i,5}D^5 = B^{i,5}$.
On the other hand a multiplication from left by D^5 scales the pth row of a matrix $C \in \mathbb{R}^{M\times M}$ if and only if $e_p \in \mathcal{E}^\delta_{h_5}$, hence $(B^{i,5})^\intercal$ is not scaled, either.
Furthermore, recall $\mathbf{l} = (\mathbf{l}^{1\intercal}, \mathbf{l}^{2\intercal}, \mathbf{l}^{4\intercal}, \mathbf{l}^{5\intercal}, \mathbf{0}^\intercal)^\intercal$, hence

$$\tilde{\mathbf{l}} = D\mathbf{l} = \begin{pmatrix} 1 & 0 & \cdots & \cdots & 0 \\ 0 & \ddots & \ddots & & \vdots \\ \vdots & \ddots & \ddots & \ddots & \vdots \\ \vdots & & \ddots & 1 & 0 \\ 0 & \cdots & \cdots & 0 & D^5 \end{pmatrix} \begin{pmatrix} \mathbf{l}^1 \\ \mathbf{l}^2 \\ \mathbf{l}^3 \\ \mathbf{l}^4 \\ \mathbf{l}^5 \\ \mathbf{0} \end{pmatrix} = \begin{pmatrix} \mathbf{l}^1 \\ \mathbf{l}^2 \\ \mathbf{l}^3 \\ \mathbf{l}^4 \\ \mathbf{l}^5 \\ \mathbf{0} \end{pmatrix} = \mathbf{l}.$$

It suffice to show that $\mathbf{u}$ as in the lemma solves the Galerkin discretized problem eq. (4.2).
Assume $\mathbf{v} \in \mathbb{R}^{N+O+M}$ solves (4.2), since A does not depend on δ, by multiplication of eq. (4.2) with D from the left and taking the limit it follows

$$\lim_{\delta\to 0} DA\mathbf{v} = \lim_{\delta\to 0} DADD^{-1}\mathbf{v} = \lim_{\delta\to 0} D\mathbf{l}.$$

Furthermore assume $\tilde{\mathbf{v}} \in \mathbb{R}^{M+O+N}$ solves (4.19g), i. e. ,

$$(\lim_{\delta\to 0} DAD)\tilde{\mathbf{v}} = \lim_{\delta\to 0} D\mathbf{l}.$$

Hence $D\tilde{\mathbf{v}}$ is a solution of eq. (4.2), $A\mathbf{u} = \mathbf{l}$.
Moreover, as shown for the right hand side $\mathbf{l}$, since D is a block diagonal matrix, whose only block not equal to the identity is the last block D^5, only the last M-rows of $\mathbf{u}$ are not equal to the entries of $\tilde{\mathbf{u}}$. □

In other words, the above lemma states, that only the entries of the stiffness matrices, which couple Raviart-Thomas elements with piecewise constant functions and the Raviart-Thomas elements among themselves are affected by the scaling.

Lemma 4.9 *The scales stiffness matrices in eq. (4.19e) are*

$$\tilde{A}^5_{p,q} = \begin{cases} \tilde{A}^{5,R_j}_{p,q} & \text{if} \quad p \neq q \quad \text{for some} \quad R_j \in \mathcal{R}_5, \\ \tilde{A}^{5,R_+(e_p)}_{p,p} + A^{5,R_-(e_p)}_{p,p} & \text{if} \quad p = q, \end{cases} \tag{4.20a}$$

$$\tilde{B}^5_{j,p} = \sum_{R\in\mathcal{R}_5, e_p\in R_j} \tilde{B}^{5,R}_p, \tag{4.20b}$$

where

$$\tilde{A}^{R_j}_{p,q} := \begin{cases} \lim_{\delta\to 0} \delta \int_{R_j} \mathbf{b}_{e_p}(\mathbf{x}) \cdot \mathbf{b}_{e_q}(\mathbf{x})\, d\mathbf{x} & \text{if} \quad e_p, e_q \in \mathcal{E}^{\delta}_{h_5}, \\ \lim_{\delta\to 0} \sqrt{\delta} \int_{R_j} \mathbf{b}_{e_p}(\mathbf{x}) \cdot \mathbf{b}_{e_q}(\mathbf{x})\, d\mathbf{x} & \text{if} \quad e_p \in \mathcal{E}^{\delta}_{h_5} \quad \text{and} \quad e_q \in \mathcal{E}^{h_5}_{h_5} \\ & \text{or} \quad e_p \in \mathcal{E}^{h_5}_{h_5} \quad \text{and} \quad e_q \in \mathcal{E}^{\delta}_{h_5}, \\ \int_{R_j} \mathbf{b}_{e_p}(\mathbf{x}) \cdot \mathbf{b}_{e_q}(\mathbf{x})\, d\mathbf{x} & \text{if} \quad e_p \in \mathcal{E}^{h_5}_{h_5} \quad \text{and} \quad e_q \in \mathcal{E}^{h_5}_{h_5} \end{cases} \tag{4.20c}$$

and

$$\tilde{B}^R_p := \begin{cases} \lim_{\delta\to 0} \sqrt{\delta} \int_R div(\mathbf{b}_{e_p})(\mathbf{x}) b_R(\mathbf{x})\, d\mathbf{x} & \text{if} \quad e_p \in \mathcal{E}^{\delta}_{h_5}, \\ \int_R div(\mathbf{b}_{e_p})(\mathbf{x}) b_R(\mathbf{x})\, d\mathbf{x} & \text{if} \quad e_p \in \mathcal{E}^{h_5}_{h_5}. \end{cases} \tag{4.20d}$$

Proof Let for $R_j \in \mathcal{R}_{h_5}$, e_p and $e_q \in \mathcal{E}_5$, $\tilde{A}^{R_j}_{p,q}$ be given as in (4.20c). On the one hand note that

$$\tilde{A}^{R_j}_{p,q} = \lim_{\delta\to 0} g(\delta, e_p, e_q) A^{5,R_j}_{p,q}(\delta, e_p, e_q),$$

for $g : \mathbb{R}^+ \times \mathcal{E}_{h_5} \times \mathcal{E}_{h_5} \to \mathbb{R}$ and on the other hand by the definition of $\tilde{A}^5$ eq. (4.19e) we have

$$\tilde{A}^5_{p,q} = \lim_{\delta\to 0} g(\delta, e_p, e_q) \int_{\Omega_5} \mathbf{b}_{e_q}(\delta, \mathbf{x}) \cdot \mathbf{b}_{e_p}(\delta, \mathbf{x}) \quad d\mathbf{x}.$$

Furthermore, using $\Omega_5 = \cup_{R_j \in \mathcal{R}} R_j$ it can be written

$$\tilde{A}^5_{p,q} = \lim_{\delta \to 0} \sum_{R_j \in \mathcal{R}_5} g(\delta, e_p, e_q) \int_{R_j} \mathbf{b}_{e_q}(\delta, \mathbf{x}) \cdot \mathbf{b}_{e_q}(\delta, \mathbf{x}) \quad d\mathbf{x},$$

moreover for $\delta > 0$ proposition 4.5 and 4.6 are valid, which shows the claim eq. (4.20a) and (4.20c). The second claim of the lemma eq. (4.20b) and (4.20d) can be shown analogously, using eq. (4.8) and proposition 4.3. □

Remark 4.10 *After taking the limit $\delta \to 0$ the virtual gap does not satisfy the cone condition.*

Practically, the virtual gap does not contain rectangles, but due to the abuse of notation, the notation is not changed, because of the limitation of the scope of this work and a simpler implementation, using standard element-wise global to local convention.
The elements of the local scaled coupling-matrices are:

Theorem 4.11 *Let $R = conv\{\mathbf{x}_1, \mathbf{x}_2, \mathbf{x}_3, \mathbf{x}_4\} \in \mathcal{R}_{h_5}$, $\mathbf{x}_1, ..., \mathbf{x}_4 \in \Theta_{h_5}$ be a rectangle, such that*

$$e_p = conv\{\mathbf{x}_p, \mathbf{x}_{p+1}\} \quad for \quad 1 \leq p \leq 4, \tag{4.21a}$$

then the local scaled stiffness matrices in the gap are

$$\tilde{A}^{5,R}_{p,q} = \begin{cases} |e_{p+1}| \left(\delta_{p,q} \frac{1}{3} + \mathbf{n}_{e_p} \cdot \mathbf{n}_{e_{p+2}} \delta_{p,q+2} \frac{1}{6} \right) & if \quad e_p \in \mathcal{E}^{\delta}_{h_5} \quad and \quad e_{p+1} \in \mathcal{E}^{h_5}_{h_5}, \\ 0 & else\ and \end{cases} \tag{4.21b}$$

$$\tilde{B}^{5,R}_{p} = \begin{cases} 1 & for \quad R = R_+(e_p), \quad e_p \in \mathcal{E}^{h_5}_{h_5} \quad and \quad e_{p+1} \in \mathcal{E}^{\delta}_{h_5}, \\ 0 & else. \end{cases} \tag{4.21c}$$

Proof The proof is build up by two parts, first eq. (4.21b) is shown and the proof of (4.21c) is left out, since it is straightforward to show it using the same technique and the fact that the normal vectors of edges of non-vanishing length is oriented outwards pointing.
Let $R \in \mathcal{R}_{h_5}$ and $e_1, ..., e_4$ be its faces. For simplification the subscript h_5 and superscript 5 is not written out in this proof.
Note due to eq. (4.20c) and (4.10b) it can be written

$$\begin{aligned} \tilde{A}^R_{p,q} = \lim_{\delta \to 0} \Big(& \delta \chi_{\mathcal{E}^\delta}(e_p) \chi_{\mathcal{E}^\delta}(e_q) + \sqrt{\delta} \chi_{\mathcal{E}^\delta}(e_p) \chi_{\mathcal{E}^{h_5}}(e_q) \\ & + \sqrt{\delta} \chi_{\mathcal{E}^{h_5}}(e_p) \chi_{\mathcal{E}^\delta}(e_q) + \chi_{\mathcal{E}^{h_5}}(e_p) \chi_{\mathcal{E}^{h_5}}(e_q) \Big) A^R_{p,q}, \end{aligned}$$

where $\chi_{\mathcal{A}}(e)$ denotes the characteristic function of the set $\mathcal{A}$. Inserting (4.10c) this equals

$$\tilde{A}^R_{p,q} = \lim_{\delta\to 0}\Big(\delta\chi_{\mathcal{E}^\delta}(e_p)\chi_{\mathcal{E}^\delta}(e_q) + \sqrt{\delta}\chi_{\mathcal{E}^\delta}(e_p)\chi_{\mathcal{E}^{h_5}}(e_q) + \sqrt{\delta}\chi_{\mathcal{E}^{h_5}}(e_p)\chi_{\mathcal{E}^\delta}(e_q) \\ \chi_{\mathcal{E}^{h_5}}(e_p)\chi_{\mathcal{E}^{h_5}}(e_q)\Big) \quad \Big(\delta_{p,q}\frac{1}{3}\frac{|R|}{|e_p|^2} + \delta_{p,q+2}\mathbf{n}_p\cdot\mathbf{n}_q\frac{1}{6}\frac{|R|}{|e_p|^2}\Big).$$

Note that, as illustrated in figure 4.5 and 4.6, due to the alignment of a rectangles in the virtual gap, it can be written

$$\frac{|R|}{|e_p|^2} = \frac{|e_{p+1}|}{\delta}\chi_{\mathcal{E}^\delta}(e_p)\chi_{\mathcal{E}^{h_5}}(e_{p+1}) + \frac{\delta}{|e_p|}\chi_{\mathcal{E}^{h_5}}(e_p)\chi_{\mathcal{E}^\delta}(e_{p+1}) \\ + \chi_{\mathcal{E}^\delta}(e_p)\chi_{\mathcal{E}^\delta}(e_{p+1}).$$

Note that A^R is a sparse matrix, whose non vanishing entries are on the main- and second off-diagonal. Therefore it suffice to calculate its elements on these diagonals. On the main diagonal the elements write as

$$\begin{aligned}\tilde{A}^R_{p,p} &= \lim_{\delta\to 0}\Big(\delta\chi_{\mathcal{E}^\delta}(e_p)\chi_{\mathcal{E}^\delta}(e_p) + \sqrt{\delta}\chi_{\mathcal{E}^\delta}(e_p)\chi_{\mathcal{E}^{h_5}}(e_p) \\ &\qquad + \sqrt{\delta}\chi_{\mathcal{E}^{h_5}}(e_p)\chi_{\mathcal{E}^\delta}(e_p) + \chi_{\mathcal{E}^{h_5}}(e_p)\chi_{\mathcal{E}^{h_5}}(e_p)\Big)A^R_{p,p} \\ &= \lim_{\delta\to 0}\Big(\delta\chi_{\mathcal{E}^\delta}(e_p) + \chi_{\mathcal{E}^{h_5}}(e_p)\Big)A^R_{p,p},\end{aligned}$$

where ist was used that $\chi_{\mathcal{E}^\delta}(e_p)\chi_{\mathcal{E}^{h_5}}(e_p) = 0$ since $\mathcal{E}^\delta \cap \mathcal{E}^{h_5} = \emptyset$ and $\chi_{\mathcal{A}}(e)\chi_{\mathcal{A}}(e) = \chi_{\mathcal{A}}(e)$. It follows inserting by inserting above formulas for $A^R_{p,p}$

$$\begin{aligned}\tilde{A}^{5,R}_{p,p} &= \lim_{\delta\to 0}\Big(\delta\chi_{\mathcal{E}^\delta}(e_p) + \chi_{\mathcal{E}^{h_5}}(e_p)\Big)\frac{1}{3}\Big(\frac{|e_{p+1}|}{\delta}\chi_{\mathcal{E}^\delta}(e_p)\chi_{\mathcal{E}^{h_5}}(e_{p+1}) \\ &\qquad + \frac{\delta}{|e_p|}\chi_{\mathcal{E}^{h_5}}(e_p)\chi_{\mathcal{E}^\delta}(e_{p+1}) + \chi_{\mathcal{E}^\delta}(e_p)\chi_{\mathcal{E}^\delta}(e_{p+1})\Big) \\ &= \frac{1}{3}|e_{p+1}|\chi_{\mathcal{E}^\delta}(e_p)\chi_{\mathcal{E}^{h_5}}(e_{p+1}).\end{aligned}$$

Because $\chi_{\mathcal{E}^\delta}(e_p)$=$\chi_{\mathcal{E}^\delta}(e_{p+2})$ for e_p and e_{p+2} opposite edges on a rectangle, it follows $\chi_{\mathcal{E}^\delta}(e_p)\chi_{\mathcal{E}^\delta}(e_{p+1}) = \chi_{\mathcal{E}^\delta}(e_p)$ and $\chi_{\mathcal{E}^{\frac{\delta}{h_5}}}(e_p)\chi_{\mathcal{E}^{\frac{h_5}{\delta}}}(e_{p+1}) = 0$, whence the entries of the second off-diagonal of $\tilde{A}^R$ are

$$\begin{aligned}\tilde{A}^R_{p,p+2} &= \lim_{\delta\to 0}\Big(\delta\chi_{\mathcal{E}^\delta}(e_p)\chi_{\mathcal{E}^\delta}(e_{p+2}) + \sqrt{\delta}\chi_{\mathcal{E}^\delta}(e_p)\chi_{\mathcal{E}^{h_5}}(e_{p+2}) \\ &\qquad + \sqrt{\delta}\chi_{\mathcal{E}^{h_5}}(e_p)\chi_{\mathcal{E}^\delta}(e_{p+2}) + \chi_{\mathcal{E}^{h_5}}(e_p)\chi_{\mathcal{E}^{h_5}}(e_{p+2})\Big)A^{5,R}_{p,p+2} \\ &= \lim_{\delta\to 0}\Big(\delta\chi_{\mathcal{E}^\delta}(e_p) + \chi_{\mathcal{E}^{h_5}}(e_p)\Big)A^R_{p,p+2}.\end{aligned}$$

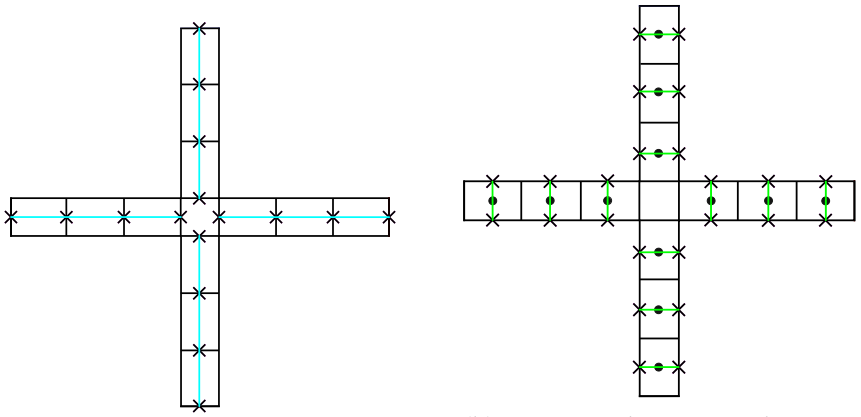

(a) Raviart-Thomas elements interaction

(b) Raviart-Thomas and piecewise constant elements interaction

Figure 4.7: Coupling edges

Furthermore, by inserting the expression for $A^R_{p,p+2}$

$$\begin{aligned}\tilde{A}^R_{p,p+2} &= \lim_{\delta\to 0}\Big(\delta\chi_{\mathcal{E}^\delta}(e_p) + \chi_{\mathcal{E}^{h_5}}(e_p)\Big)\mathbf{n}_p\cdot\mathbf{n}_{p+2}\frac{1}{6}\Big(\frac{|e_{p+1}|}{\delta}\chi_{\mathcal{E}^\delta}(e_p)\chi_{\mathcal{E}^{h_5}}(e_{p+1}) \\ &\quad + \frac{\delta}{|e_p|}\chi_{\mathcal{E}^{h_5}}(e_p)\chi_{\mathcal{E}^\delta}(e_{p+1}) + \chi_{\mathcal{E}^\delta}(e_p)\chi_{\mathcal{E}^\delta}(e_{p+1})\Big) \\ &= \mathbf{n}_p\cdot\mathbf{n}_{p+2}\frac{1}{6}|e_{p+1}|\chi_{\mathcal{E}^\delta}(e_p)\chi_{\mathcal{E}^{h_5}}(e_{p+1}).\end{aligned}$$

Therefore the local scaled stiffness matrix is given by

$$\tilde{A}^R_{p,q} = \Big(\delta_{p,q}\frac{1}{3} + \delta_{p,q+2}\mathbf{n}_{e_p}\cdot\mathbf{n}_{e_q}\frac{1}{6}\Big)|e_{p+1}|\chi_{\mathcal{E}^\delta}(e_p)\chi_{\mathcal{E}^{h_5}}(e_{p+1}). \qquad \square$$

Since by eq. (4.21c) the local $\mathcal{RT}_0$ stiffness matrix vanishes on $R_-(e_p)$, eq. (4.20b) reduces to:

Lemma 4.12 *The global scaled stiffness matrix of Raviart-Thomas and piecewise consonant finite elements writes as*

$$\tilde{B}^5_{j,p} = \begin{cases} 1 & \text{if} \quad e_p \in \mathcal{E}^{h_5}_{h_5} \quad \text{and} \quad |R_j| \neq 0 \\ 0 & \text{if} \quad \text{else} \end{cases} \tag{4.22}$$

By the above theorem it follows from the stencil of the stiffness matrices, that the following shape functions couple through the stiffnessmtarix $\tilde{A}$:

$\mathcal{RT}_0$-**Self-Interaction**

- Contributions to the stiffness matrix are associated to the edges of vanishing length.
- Interaction of parallel edges of vanishing length
- There is no contribution of the small square.
- The order of the coupling is proportional to the length of non vanishing edges.

$\mathcal{RT}_0$-W_0-**Coupling**

- Interaction of edges of vanishing length with the neighboring elements
- Contributions are independent of mesh width.
- No contribution of the small square and zero row in the local stiffness matrix if the small square is incorporated.

The interacting edges and elements in the gap are illustrated in figure 4.7.

$\mathcal{RT}_0$-$S^1_{0;\partial\Omega\setminus\Gamma}$-**Coupling** Furthermore by eq. (4.4) and (4.5) it is concluded:

- Contributions of stiffness matrix are associated to edges of non vanishing length.
- Order of coupling is inverse proportional to the the length of non-vanishing edges.
- Order of coupling is maximal if a virtual edge contains the edge of a triangle.

4.4 Scaled Stiffness Matrix Example

The stiffness matrix block $\tilde{A}^5$of the scaled Galerkin problem eq. (4.19g) for the mesh illustrated in figure 4.8 are given below. The edges' and vertices' indexes, edges' orientations of the primal mesh are given in figure 4.8b.
The coordinates are given by the file `Coord_square_I_01_5_3.dat`, which uses the LehrFEM class of a mesh coordinates and can be found in appendix A.2. Vanishing matrix elements are not listed.
In the example we have $|e| = \frac{1}{4}$ for all $e \in \mathcal{E}^{h_5}_{h_5}$ and the entries of the $\mathcal{RT}_0$-

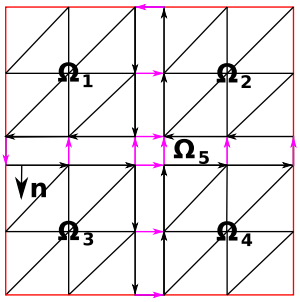

(a) Primal and dual mesh

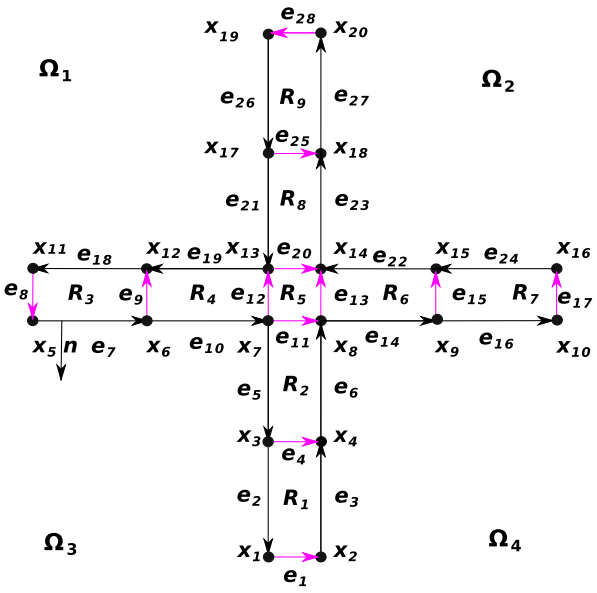

(b) Elements, vertecies and edges of $\mathcal{R}_5$

Figure 4.8: Compatible meshes

$\mathcal{RT}_0$-stiffness matrix are

$$\tilde{A}^5_{1,1} = \frac{1}{3}|e_3| = \frac{1}{3}\frac{1}{4} = \frac{1}{12} = 0.08\bar{3}, \tag{4.23a}$$

$$\tilde{A}^5_{1,4} = \tilde{A}^5_{4,1} = \frac{1}{6}|e_3| = \frac{1}{6}\frac{1}{4} = \frac{1}{24} = 0.041\bar{6}, \tag{4.23b}$$

$$\begin{aligned}\tilde{A}^5_{4,4} &= \tilde{A}^{5,R_1}_{4,4} + \tilde{A}^{5,R_2}_{4,4} = \frac{1}{3}|e_3| + \frac{1}{3}|e_6| = \frac{1}{3}\frac{1}{4} + \frac{1}{3}\frac{1}{4} = \frac{1}{6} \\ &= 0.1\bar{6}, \end{aligned} \tag{4.23c}$$

$$\tilde{A}^5_{4,11} = \tilde{A}^5_{11,4} = \frac{1}{3}|e_6| = \frac{1}{3}\frac{1}{4} = \frac{1}{12} = 0.041\bar{6}, \tag{4.23d}$$

$$\tilde{A}^5_{11,11} = \frac{1}{3}|e_5| = \frac{1}{3}\frac{1}{4} = \frac{1}{12} = 0.08\bar{3}, \tag{4.23e}$$

$$\tilde{A}^5_{8,8} = \tilde{A}^5_{1,1} = 0.08\bar{3} \quad \text{due to symmtery of the mesh,} \tag{4.23f}$$

$$\tilde{A}^5_{8,9} = \tilde{A}^5_{9,8} = -\tilde{A}^5_{1,4} = -0.041\bar{6} \quad \text{due to symmtery of the mesh,} \tag{4.23g}$$

$$\tilde{A}^5_{9,9} = \tilde{A}^5_{4,4} = 0.1\bar{6} \quad \text{due to symmtery of the mesh,} \tag{4.23h}$$

$$\tilde{A}^5_{9,12} = \tilde{A}^5_{4,11} = 0.041\bar{6} \quad \text{due to symmtery of the mesh,} \tag{4.23i}$$

$$\tilde{A}^5_{12,12} = \frac{1}{3}|e_{19}| = \frac{1}{3}\frac{1}{4} = \frac{1}{12} = 0.08\bar{3}, \tag{4.23j}$$

$$\tilde{A}^5_{13,13} = \frac{1}{3}|e_{13}| = \frac{1}{3}\frac{1}{4} = \frac{1}{12} = 0.08\bar{3}, \tag{4.23k}$$

$$\tilde{A}^5_{13,15} = \tilde{A}^5_{15,13} = \frac{1}{6}|e_{14}| = \frac{1}{6}\frac{1}{4} = \frac{1}{24} = 0.041\bar{6}, \tag{4.23l}$$

$$\tilde{A}^5_{15,15} = \tilde{A}^{R_6}_{15,15} + \tilde{A}^{R_7}_{15,15} = \frac{1}{3}|e_{14}| + \frac{1}{3}|e_{16}| = \frac{2}{3}\frac{1}{4} = \frac{1}{6} = 0.1\overline{6}, \tag{4.23m}$$

$$\tilde{A}_{15,17} = \tilde{A}_{17,15} = \frac{1}{6}|e_{16}| = \frac{1}{6}\frac{1}{4} = \frac{1}{24} = 0.041\overline{6}, \tag{4.23n}$$

$$\tilde{A}^5_{17,17} = \frac{1}{3}|e_{24}| = \frac{1}{3}\frac{1}{4} = \frac{1}{12} = 0.08\overline{3}, \tag{4.23o}$$

$$\tilde{A}^5_{20,20} = \tilde{A}_{13,13} = 0.08\overline{3} \quad \text{due to symmtery of the mesh,} \tag{4.23p}$$

$$\tilde{A}^5_{20,25} = \tilde{A}_{13,15} = 0.041\overline{6} \quad \text{due to symmtery of the mesh,} \tag{4.23q}$$

$$\tilde{A}^5_{25,25} = \tilde{A}^5_{15,15} = 0.1\overline{6} \quad \text{due to symmtery of the mesh,} \tag{4.23r}$$

$$\tilde{A}^5_{25,28} = \tilde{A}^5_{28,25} = -\tilde{A}^5_{15,17} = -0.041\overline{6} \quad \text{due to} \tag{4.23s}$$

symmtery of the mesh and

$$\tilde{A}^5_{28,28} = \tilde{A}^5_{17,17} = 0.08\overline{3} \quad \text{due to symmtery of the mesh.} \tag{4.23t}$$

4.5 Applicability of the Virtual Gap Method

The virtual gap method is applicable to partitions different from partition I and a variate of meshes using LehrFEM as examined here.

First, note that no matching condition on the primal and dual mesh was required in the proof of theorem 4.11 and therefore the imposed result is applicable to non conforming primal and dual meshes. Non conforming meshes are given, whenever the vertices of the joint boundary of two meshes do not coincide. Furthermore, the stiffness matrices stencil are independent of the triangularization, hence in implementations non shape regular dual meshes are admissible. Also there is no need of a uniform primal mesh, because the length of non-vanishing edges is arbitrary. Note that this enables non-uniform mesh refinements, using an error-adaptive refinement procedure. Non uniform, non conforming elements are illustrated in figure 4.9.

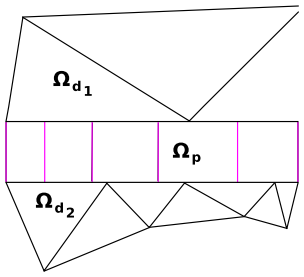

Figure 4.9: Non conforming, non uniform meshes

Second, it sufficed to use the orthogonality and parallelism of primal edges and a partition of the set of edges due to their length in the proof of theorem

4.11, hence the primal mesh does not have to be aligned with the coordinate axes of the domain Ω. The author suggests that a similar result can be derived for different shapes of the virtual gap as for example in figure 4.10 by slight modifications of the proof.

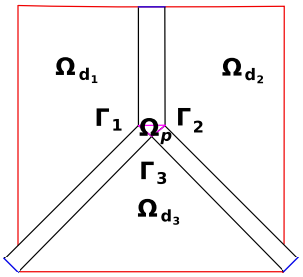

Figure 4.10: Alternative partition of the domain

Moreover, the assembly in an implementation of the stiffness matrix is straight forward using standard local to global technique as imposed in LehrFEM [4, chp. 4], e. g. element- and boundary flags in order to distinguish edges, elements and nodes. Since the primal mesh's orientation is non trivial in the assembly of the stiffness matrix, a counterclockwise alignment of the primal boundary edges is of necessity. The data struct `mesh` found in LehrFEM, can be easily modified by a simple routine, such that the primal mesh's boundary is orientated. Additionally LehrFEM already provides the variable `Edge2Elem`, connecting edges to their neighboring elements. In particular, note that $R = R_+(e)$ if and only if R is the right neighboring element of the edge e.

Chapter 5

Conclusion

In this work Laplace equation with a Dirichlet boundary condition is investigated. It is specified the primal-dual problem, by spiting the domain of definition and equipping the primal variable with a Dirichlet boundary condition, respectively the dual variable with a Neumann boundary condition, on the joint boundary as in [15]. It is formulated as weak solution, the saddel point problem.

Since a conforming mixed FEM-method is sought to be used, the continuity assumptions of the underlying polynomial spaces, differ for the three types of FEM imposed in this work. The functions in $S^k_{0,\Gamma}(\Omega, \mathcal{T})$ are continuous and square integrable on the domain of definition. The traces of normal components of $\mathbf{P}^k_{\mathbf{k}+\mathbf{x}k}(R)$ lie in $R_k(\partial R)$, therefore $\mathcal{RT}_0(\Omega, \mathcal{R})$ functions restriction on edges of bilinear elements are polynomials, while the functions itself lie in $L^2(\Omega)^2$ and their divergence in $L^2(\Omega)$. Furthermore elements of $W_k(\Omega, \mathcal{R})$ are not continuous, but polynomials on elements and L^2 on Ω. In contrast to $W_0(\Omega, \mathcal{R})$ and $S^k_{0;\Gamma}(\Omega, \mathcal{T})$, for $\mathcal{RT}_0(\Omega, \mathcal{R})$ the conformingness is given by an local assumption on element boundaries, while W_0 and $S^k_{0;\Gamma}$ confomingness is ensured by an assumption on a global property on the whole domain of definition.
By transformation of elements to the reference element a basis was constructed for conforming affine triangular linear FEM, $\Pi = P^1(T)$, and piecewise constant finite elements, $\Pi = P^0(R)$, following [11] and [3] and conforming affine bilinear $\mathcal{RT}_0$ FEM, i. e. , $\Pi = \mathbf{P}^0_{\mathbf{0}+\mathbf{x}0}(R)$, using the ideas in [1]. These basis functions are barycentric coordinates, the standard basis of $W_0(\Omega, \mathcal{R})$, and the roof functions. Basis function of conforming linear FEM are constructed from a basis on a single triangle, by defining patches such that single basis functions are assembled by literally resembling nodes, such that the overall function is continuously put together on the boundary of single triangles, which contribute the patch. On the other hand, reassembling nodes and therefore constructing basis functions of conforming $\mathcal{RT}_0$-

elements by using a Lagrangian type condition on the normal components is not possible. Because, if a basis function of an edge fulfills a Lagrangian type interpolation property like theorem 3.19, i) this leads to basis' normal component, which is parallel to the edges normal vector and vanishes, since the linear part of the function has a zero on the element's opposite edge. This kind of roof shaped shape function can not be rotated on other rectangular elements by resembling nodes. In particular this is due to the fact, that affine transformations do not transform the normal components of basis functions, since it only acts on the linear part and not the direction of a vector valued function.
The transformation mapping normal components of the reference rectangle to an arbitrary rectangular element is a special (contravariant) transformation known as Piola transformation [2, chp. 2.1.3]. No Piola transformations was used in this work, hence the proof of theorem 3.19 is comprehensible for readers, who are not familiar with differential geometry. Since there is no overall global continuity assumption on $H(div;\Omega)$ unless square integrability, which is true for piecewise polynomials anyway, this proof uses techniques, that are natural.
In the next step (sec. 4.1) Poisson's problem was discretized, using a dual domain contributing of multiple, non adjacent components. The two mixed type BVPs are rebind by Green's formula and partial integration, due to the flux propagating through the joint boundary and a transmitting Dirichlet BC. Applying a Galerkin discretization, a symmetric linear system is derived for the degrees of freedom. Due to the separation of the dual sub domain by the joint boundary block matrices, corresponding to the degrees' of freedom coupling in the primal and dual mesh, occur. The calculated stiffness matrix blocks are the standard linear FEM with mixed Dirichlet BC element matrix (eq. (4.2d)), the $\mathcal{RT}_0$ element matrix (eq. (4.2f)), and the mixed element matrices of piecewise constant FEM and $\mathcal{RT}_0$-FEM (eq. (4.2h)), of linear FEM and $\mathcal{RT}_0$-FEM (eq. (4.2g)). The right hand side contributes of l^i, the standard LFE load vector, and the negative load vector of piecewise constant FEM, l^5 (see eq. (4.2e) and (4.2i)). Using LehrFEM they can be implemented by the function `assemLoad_LFE` and a two dimensional quadrature rule [4, chp. 5.2].
Assuming a virtual gap of infinitesimal width the $\mathcal{RT}_0(\Omega,\mathcal{R})$ basis functions scale, wherefore the stiffness matrix is diagonal transformed to prevent a blowup. Due to the scaling, entries of the stiffness matrix vanish, but LFE-$\mathcal{RT}_0$ coupling is not effected. In blocks of the stiffness matrix matrix elements vanish, depending on if the edges are of vanishing or non vanishing length. These elements depend on the edge length, not on edge length or the length of the intersection of primal and dual edges. The small square does not add a contribution, as expected by modeling an infinitesimal wide primal domain.
The results can be easily generalized to non coordinate axis aligned virtual

gaps. The work is applicability for a implementation in MATLAB using LehrFEM, due to the results local representation.
Nevertheless it remains open in this work if the method converges, since the convergence result by [15] is not straight forward applicable to bilinear FEM. Also since the virtual gap of vanishing width does not satisfy the cone condition, the existence of a solution of Poisson's equation on partition I for a vanishing virtual gap can not be stated in this work.

5.1 Future Works

Because the numerical experiments could not be finished it is planed to finalize the implementation build up on LehrFEM. Also the intermediate results are not documented jet. Once the results of this work are implemented, the implementation can be adapted to other partitions of the domain Ω for different right hand sides f of Poisson's equation, multiple mesh widths, non uniform meshes, matching and non matching primal and dual meshes, etc.
.
Furthermore the virtual gap method can be generalized for a three dimensional domain of definition.
Beside that, there are many more ways, how this work can be pursued. More theoretical aspects of the primal dual virtual gap method can be elaborated. Textbooks can be consulted about the nature of the space $H(\mathrm{div};\Omega)$, in order to give the functional analysis frame work of this space and exploring convergence results. The convergence of the scheme can be examined, by consulting the literature for saddle point problems. Also the properties and structure of the scaled stiffness matrix can be analyzed and related to application's material properties and convergence.

Appendix A

Appendix

A.1 Weak Formulation of Poission's Equation

Find $(\mathbf{j_p}, u_p, u_d) \in H(\mathrm{div};\Omega_p) \times L^2(\Omega_p) \times H^1_{0;\Gamma_d}(\Omega_d)$ such that

$$\int_{\Omega_p} \mathbf{j}_p \cdot \mathbf{q}_p \, d\mathbf{x} + \int_{\Omega_p} \mathrm{div}(\mathbf{q}_p) u_p \, d\mathbf{x} - \int_{\Gamma} \mathbf{q}_p u_d \cdot \mathbf{n} \, d\sigma(\mathbf{x}) = 0, \quad \text{for all} \quad \mathbf{q}_p \in H(\mathrm{div};\Omega_p), \tag{A.1a}$$

$$\int_{\Omega_p} \mathrm{div}(\mathbf{j}_p) v_p \, d\mathbf{x} = -\int_{\Omega_p} f v_p \, d\mathbf{x}, \quad \text{for all} \quad v_p \in H^0(\Omega_p) \quad \text{and} \tag{A.1b}$$

$$-\int_{\Gamma} \mathbf{j}_p v_d \cdot \mathbf{n} \, d\sigma(\mathbf{x}) - \int_{\Omega_p} \nabla u_d \cdot \nabla v_d \, d\mathbf{x} = -\int_{\Omega_d} f v_d \, d\mathbf{x}, \quad \text{for all} \quad v_d \in H^1_{0;\Gamma_d}(\Omega_d). \tag{A.1c}$$

A.2 Mesh Coordinates `Coord_square_I_01_5_3.dat`

`Coord_square_I_01_5_3.dat`

```
% List of vertices
%
%   User  :  Tanja Almeroth
%   Date  :  21.11.16
%
%   The first column contains the global index of
   each vertex.
%
% Setup I, Omega_5
```

```
1       +0.500000e+00  +0.000000e+00
2       +0.500000e+00  +0.000000e+00
3       +0.500000e+00  +0.250000e+00
4       +0.500000e+00  +0.250000e+00
5       +0.000000e+00  +0.500000e+00
6       +0.250000e+00  +0.500000e+00
7       +0.500000e+00  +0.500000e+00
8       +0.500000e+00  +0.500000e+00
9       +0.750000e+00  +0.500000e+00
10      +1.000000e+00  +0.500000e+00
11      +0.000000e+00  +0.500000e+00
12      +0.250000e+00  +0.500000e+00
13      +0.500000e+00  +0.500000e+00
14      +0.500000e+00  +0.500000e+00
15      +0.750000e+00  +0.500000e+00
16      +1.000000e+00  +0.500000e+00
17      +0.500000e+00  +0.750000e+00
18      +0.500000e+00  +0.750000e+00
19      +0.500000e+00  +1.000000e+00
20      +0.500000e+00  +1.000000e+00
```

Bibliography

[1] C. Bahriawati and C. Carstensen. Three MATLAB Implementations of the lowest-order Raviart-Thomas MFEM with a posteriori Error Control. *Computaional Methods in Applied Mathematics*, 5(4):333–361, 2005.

[2] D. Boff, F. Brezzi, and M. Forti. *Mixed Finite Element Methods and Applications*, volume 44 of *Springer Series in Computational Mathematics*. Springer Berlin Heidelberg, 2013.

[3] D. Braess. *Finite Elemente*, volume 5. Springer Berlin Heidelberg, 2013.

[4] A. Burtscher, E. Fonn, and P. Meury. *LehrFEM - A 2D Finite Element Toolbox*. Homepage, March 2012. available online at https://svn.id.ethz.ch/sam/Numcourses/rw/matlab/LehrFEM/LehrFEM_minimal.zip, downloaded at 28. September 2016.

[5] X. Claeys and R. Hiptmair. Boundary integral formulation of the first kind for acoustic scattering by composite structures. Technical Report 2011-45, Seminar for Applied Mathematics, ETH Zürich, Switzerland, 2011.

[6] W. Greiner. *Classical Electrodynamics*, volume 1. Springer Berlin Heidelberg, 1998.

[7] P. Ledger and R. Hiptmair. A quadrilateral edge element scheme with minimum dispersion. Technical Report 2003-17, Seminar for Applied Mathematics, ETH Zürich, Switzerland, 2003.

[8] B. Q. Li. *Discontinuous finite elements in fluid dynamics and heat transfer*. Springer, 2006.

[9] P. E. Meury. *Stable finite element boundary element Galerkin schemes for acoustic and electromagnetic scattering*. PhD thesis, Eidgenössische Technische Hochschule ETH Zürich, 2007.

[10] K. Noor. Books and monographs on finite element technology. *Finite Elements in Analysis and Design 1*, 1(1):101–111, 1985.

[11] S. Sauter. *Numerische Methoden für elliptische und parabolische Differentialgleichungen, Version 16. Dezember 2014*. Homepage, 2014. available online at http://www.math.uzh.ch/index.php?file&key1=29580, downloaded at 18. December 2014.

[12] J. Smajic. *How to electromagnetic finite element analysis*. Hamilton, 2006.

[13] G. Strang. Approximation in the finite element method. *Numerische Mathematik*, 19:81–98, 1971.

[14] G. Strang and A. E. Berger. *The change in solution due to change in domain*, volume 23 of *Proceedings of Symposia in Pure Mathematics*. Americal Mathematical Society, 1973.

[15] C. Wieners and B. I. Wohlmuth. The coupling of mixed and conforming finite element discretizations. In *Contemporary Mathematics*, volume 218, pages 547–554. American Mathematical Society, 1998.

[16] P. Wriggers. *Nonlinear Finite Element Methods*, volume 1. Springer Berlin Heidelberg, 2008.

[17] M. Zlámal. On the finite element method. *Numerische Mathematik*, 12:394–409, 1968.

Eidgenössische Technische Hochschule Zürich
Swiss Federal Institute of Technology Zurich

Declaration of originality

The signed declaration of originality is a component of every semester paper, Bachelor's thesis, Master's thesis and any other degree paper undertaken during the course of studies, including the respective electronic versions.

Lecturers may also require a declaration of originality for other written papers compiled for their courses.

I hereby confirm that I am the sole author of the written work here enclosed and that I have compiled it in my own words. Parts excepted are corrections of form and content by the supervisor.

Title of work (in block letters):

Mixed bilinear Raviart-Thomas and triangular linear finite elements virtual gap technique applied to Poission's equation

Authored by (in block letters):

For papers written by groups the names of all authors are required.

Name(s):	**First name(s):**
Almeroth	Tanja

With my signature I confirm that

- I have committed none of the forms of plagiarism described in the 'Citation etiquette' information sheet.
- I have documented all methods, data and processes truthfully.
- I have not manipulated any data.
- I have mentioned all persons who were significant facilitators of the work.

I am aware that the work may be screened electronically for plagiarism.

Place, date	**Signature(s)**
Zürich,31.12.16	Tanja Almeroth

For papers written by groups the names of all authors are required. Their signatures collectively guarantee the entire content of the written paper.